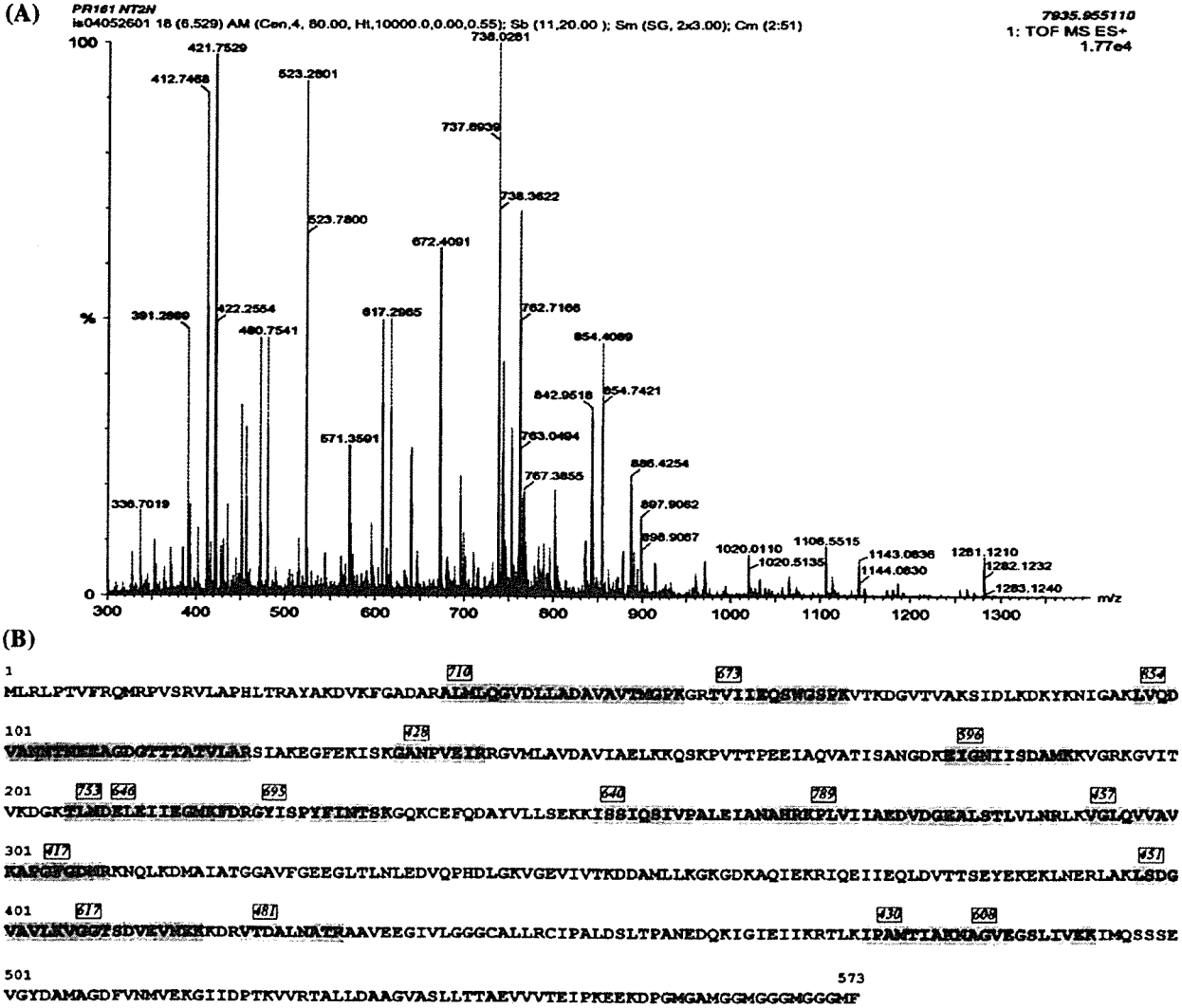

FIGURE 2. Mass spectrometric analysis of the 14-3-3-binding protein in NTera2-N cells. Spot 1 labeled with the rh14-3-3ζ probe (Fig. 1) was excised from the gel, trypsinized, and processed for nanoESI-MS/MS analysis. **(A)** The spectra of MS analysis. Each peak indicates individual peptide fragments. The positions of several peaks were automatically numbered on the spectra. The fragments were selected for MS analysis in order of their signal intensity, although autolytic fragments of trypsin (e.g. 412, 421, 523, 737, 762, and 767) were omitted. **(B)** Amino acid sequence of human Hsp60. Seventeen peptide fragments of spot 1 identified by MS analysis (shadowed) showed a perfect match with the sequence encompassing amino acid residues 38–493 of human Hsp60. The number indicated on each fragment represents the position in the horizontal axis of the spectra.

Immunoprecipitation Analysis

To express recombinant human proteins in cultured cells, the PCR product was cloned into a mammalian expression vector pcDNA4/HisMax-TOPO (Invitrogen) to produce a fusion protein with an N-terminal Xpress tag. The vector was transfected in HEK293 cells by Lipofectamine 2000 reagent (Invitrogen).

To prepare total protein extract for immunoprecipitation (IP) analysis, cells and tissues were homogenized in M-PER lysis buffer (Pierce, Rockford, IL) with a cocktail of protease inhibitors and phosphatase inhibitors (Sigma) followed by centrifugation at 12,000 rpm at 4°C for 20 minutes. After preclearance, the supernatant was incubated at 4°C for 3 hours with 30 μg/mL rabbit polyclonal anti-14-3-3 protein antibody (K19)-conjugated agarose (Santa Cruz Biotechnology) or the same amount of normal rabbit IgG-conjugated agarose (Santa Cruz Biotechnology). After several washes, the immunoprecipitates were processed for Western blot analysis using anti-HSP60 antibody (N-20), mouse monoclonal, anti-prion protein antibody (3F4; Dako, Carpinteria, CA), mouse monoclonal anti-14-3-3 protein antibody (H-8; Santa Cruz Biotechnology), or anti-Xpress antibody.

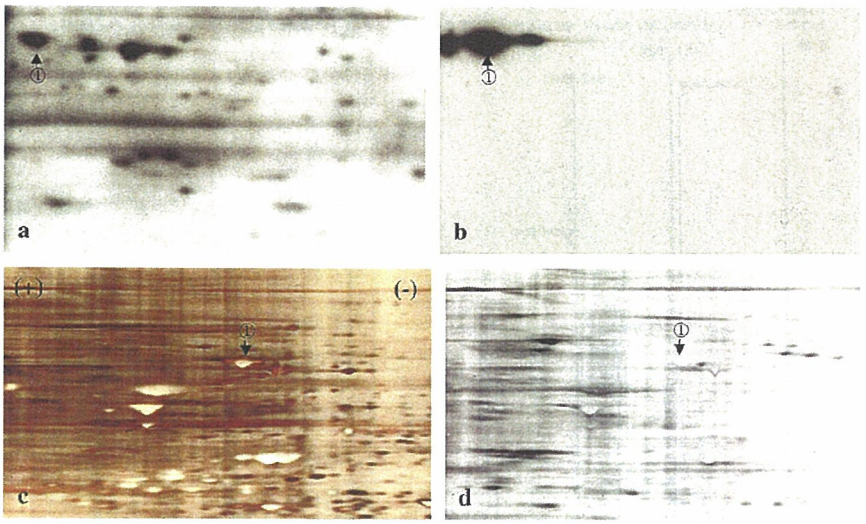

FIGURE 3. The interaction of 14-3-3 protein with Hsp60 was not zeta isoform-specific. Two hundred micrograms of total cellular protein of NTera2-N was separated on a 2-dimensional PAGE gel ([a, b]: pI 5.3–6.3 and 4%–12%; [c, d]: pI 4–7 and 4%–12%), followed by silver staining or phosphoprotein staining. The gel was processed for overlay with recombinant human 14-3-3γ protein (rh14-3-3γ) tagged with Xpress, followed by relabeling with anti-Hsp60 antibody. **(a)** rh14-3-3ζ, **(b)** Hsp60, **(c)** silver staining, **(d)** phosphoprotein staining. Spot 1 is indicated by an arrow.

Immunocytochemistry and Immunohistochemistry

For double-labeling immunocytochemistry, cells plated on cover glasses were fixed with 4% paraformaldehyde in 0.1 M phosphate buffer (pH 7.4) at RT for 10 minutes followed by incubation with phosphate-buffered saline (PBS) containing 0.5% Triton X-100 at RT for 20 minutes and with PBS containing 10% normal human serum at RT for 15 minutes. In some experiments, live cells were labeled with MitoTracker Red CMXRos (Molecular Probes) before fixation. The cells were then incubated at RT for 30 minutes with anti-HSP60 antibody (N-20) followed by incubation with Rhodamine Red-X-conjugated anti-goat IgG (Jackson ImmunoResearch, West Grove, PA). They were then incubated with rabbit anti-14-3-3ζ isoform antibody (IBL, Gumma, Japan) or mouse monoclonal anti-prion protein antibody (8G8; Cayman Chemical, Ann Arbor, MI) followed by incubation with Alexa Fluor 488-conjugated anti-rabbit or anti-mouse IgG (Molecular Probes). In limited experiments, the cells were incubated at RT for 5 minutes with 4′,6′-diamidino-2-phenylindole (DAPI) (1:30,000; Molecular Probes). After several washes, cover glasses were mounted on the slides with glycerol–polyvinyl alcohol and examined under a Nikon ECLIPSE E800 universal microscope. Negative controls were processed following these steps except for exposure to primary antibody.

For immunohistochemistry, 10-μm-thick serial sections were prepared from several autopsy brains of multiple sclerosis and cerebral infarction. Detailed clinical profiles of the patients were described previously (26). The brains were fixed with 4% paraformaldehyde and embedded in paraffin. After deparaffination, the tissue sections were heated by microwave at 95°C for 10 minutes in 10 mM citrate sodium buffer (pH 6.0) followed by incubation at RT for 15 minutes with 3% H_2O_2-containing methanol. For prion protein immunolabeling, the sections were pretreated by boiling for 20 minutes in the citrate sodium buffer according to the methods described previously (27). The tissue sections were then incubated with PBS containing 10% normal goat or rabbit serum at RT for 15 minutes to block nonspecific staining. They were then incubated at 4°C overnight with anti-14-3-3ζ isoform antibody (IBL), anti-HSP60 antibody (N-20), anti-prion protein antibody (8G8), rabbit anti-glial fibrillary acidic protein (GFAP) antibody (N1506; Dako), or rabbit anti-neuron-specific enolase (NSE) antibody (Nichirei, Tokyo, Japan). After washing with PBS, the tissue sections were labeled at RT for 30 minutes with peroxidase-conjugated secondary antibodies (Simple Stain MAX-PO kit, Nichirei) followed by incubation with a colorizing solution containing diaminobenzidine tetrahydrochloride (DAB) and a counterstain with hematoxylin. For negative controls, the sections were incubated with a negative control reagent (Dako) instead of primary antibodies.

RESULTS

Identification of Hsp60 as a 14-3-3-Binding Protein in Human Neurons

To identify 14-3-3-binding proteins in human neurons, we performed a protein overlay analysis using recombinant human 14-3-3ζ protein (rh14-3-3ζ) tagged with Xpress as a probe. Total protein extract of NTera2-derived differentiated neurons (NTera2-N) was separated on a 2D-PAGE gel and transferred onto a PVDF membrane (Fig. 1). The rh14-3-3ζ probe reacted strongly with several spots on the blot, among which a major 60-kDa spot was designated spot 1 (Fig. 1b). In contrast, the rhISG15 probe did not label any of these spots, excluding nonspecific binding of rh14-3-3ζ through the Xpress tag (Fig. 1d). Spot 1 was excised from the original gel, trypsinized, and processed for nanoESI-MS/MS analysis (Fig. 2A). Seventeen peptide fragments derived from the spot 1 showed a perfect match with the sequence covering amino acid residues 38–493 of human Hsp60 (Fig. 2B). This indicates that spot 1 corresponds to the nearly full length of Hsp60. Anti-Hsp60 antibody labeled spot 1, verifying the results (Fig. 1c). Furthermore, the rh14-3-3γ probe also

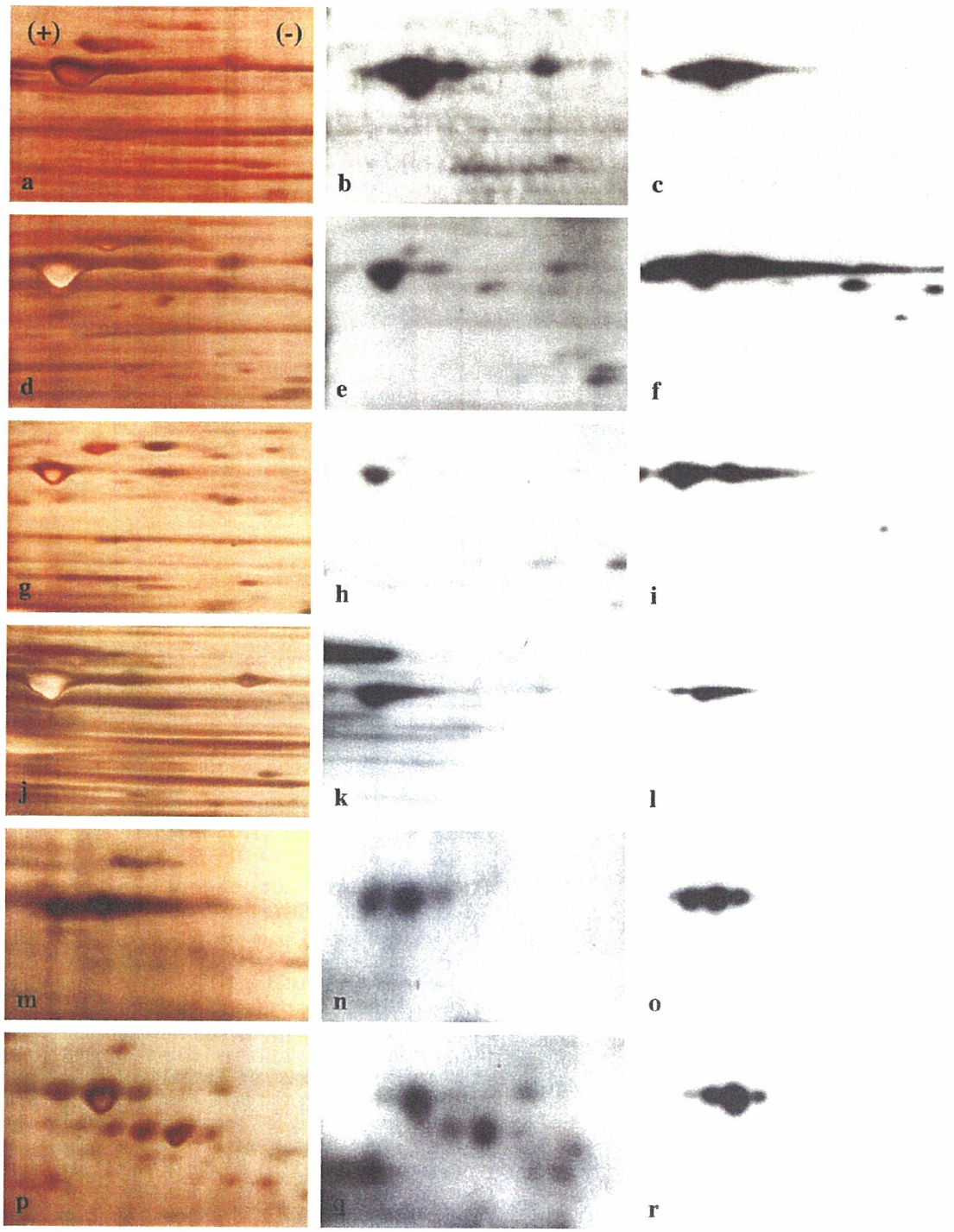

FIGURE 4. The interaction of 14-3-3 protein with Hsp60 was universal in neuronal and nonneuronal cells. Two hundred micrograms of total cellular protein of human cell lines and brain homogenate was separated on a 2-dimensional PAGE gel ([**a–l**]: pI 5.3–6.3 and 4% to 12%; [**m–r**]: pI 4-7 and 4% to 12%) followed by silver staining (the left panels). The gel was processed for overlay with the rh14-3-3ζ probe tagged with Xpress or Myc (the center panels) followed by relabeling with anti-Hsp60 antibody (the right panels). **(a–c)** Undifferentiated NTera2 teratocarcinoma (NTera2-U), **(d–f)** SK-N-SH neuroblastoma, **(g–i)** U-373MG astrocytoma, **(j–l)** HeLa cervical carcinoma, **(m–o)** human neuronal progenitor (NP) cells, **(p–r)** brain homogenate.

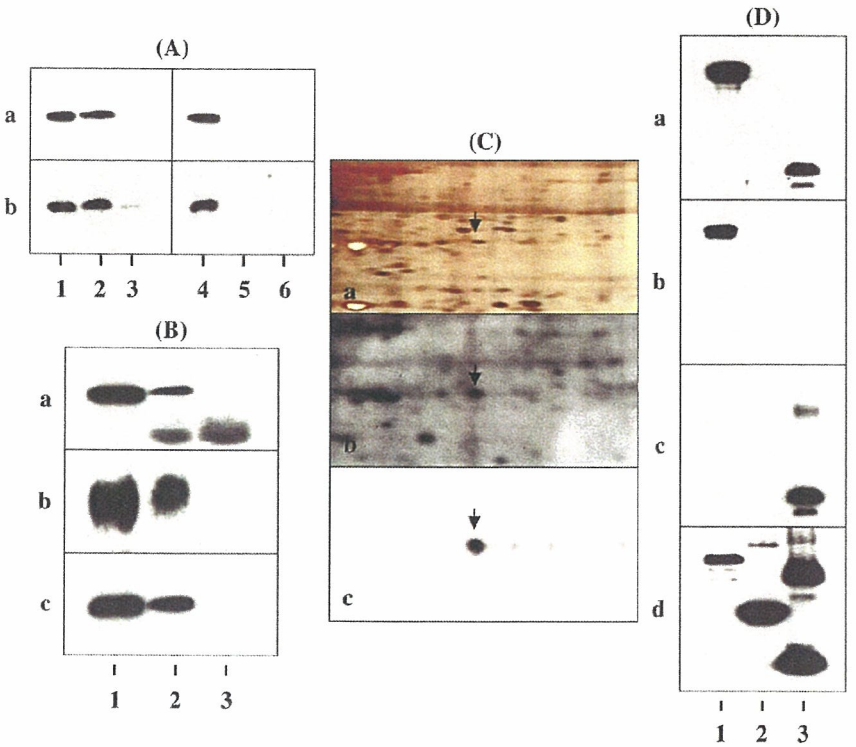

FIGURE 5. The interaction of 14-3-3 protein with both Hsp60 and PrPC. **(A)** The 14-3-3-binding domains of Hsp60 and PrPC. Either the N-terminal half (NTF) (lanes 1–3) or the C-terminal half (CTF) (lanes 4–6) of (a) recombinant human HSP60 or (b) PrPC tagged with Xpress was separately expressed in HEK293 cells. The cellular protein extract was processed for immunoprecipitation (IP) with (2, 5) anti-14-3-3 protein antibody (K-19) or (3, 6) rabbit IgG, followed by immunoblotting with anti-Xpress antibody. The lanes (1, 4) indicate the input control. **(B)** Coimmunoprecipitation of 14-3-3 with Hsp60 and PrPC. Human brain homogenate was processed for IP with (2) K-19 or (3) rabbit IgG followed by immunoblotting with (a) anti-Hsp60 antibody (N-20), (b) anti-prion protein antibody (3F4), or (c) anti-14-3-3 protein antibody (H8). Lane (1) indicates the input control. **(C)** The interaction of 14-3-3 with PrPC. Two hundred micrograms of human brain protein extract was separated on a 2-dimensional PAGE gel (pI 4–7 and 4%–12%), silver-stained, and processed for overlay with the rh14-3-3ζ probe tagged with Myc followed by relabeling with anti-prion protein antibody (3F4). (a) Silver staining, (b) rh14-3-3ζ, (c) PrPC. **(D)** Phosphorylation-independent interaction of 14-3-3 with Hsp60 and PrPC. Xpress-tagged recombinant proteins of (1) human Hsp60, (2) LacZ fragment, and (3) human PrPC produced by *Escherichia coli* were processed for overlay with (a) the rh14-3-3ζ probe tagged with Myc, followed by relabeling with (b) anti-Hsp60 antibody (N-20), (c) anti-prion protein antibody (3F4), or (d) anti-Xpress antibody.

reacted with spot 1, suggesting that the interaction of 14-3-3 with Hsp60 is not ζ isoform-specific (Fig. 3a, b). Hsp60 does not possess a substantial amount of phosphorylated amino acid residues, because spot 1 was not labeled by the phosphoprotein gel stain (Fig. 3c, d).

To study whether the interaction of 14-3-3 with Hsp60 is a neuron-specific event, protein extracts of undifferentiated NTera2 (NTera2-U), SK-N-SH neuroblastoma, U-373MG astrocytoma, HeLa cervical carcinoma, human NP cells, and human brain homogenate were separated on a 2D-PAGE gel and processed for protein overlay with the rh14-3-3ζ probe tagged with Xpress or Myc. This identified Hsp60 as a universal binding partner for the 14-3-3 protein (Fig. 4a–r).

The 14-3-3-Interacting Domain Was Located in N-Terminal Half of Hsp60

To identify the 14-3-3-binding site of Hsp60, either the N-terminal half with cleavage of the mitochondrial import signal (NTF; amino acid residues 27–287) or the C-terminal half (CTF; amino acid residues 288–573) of human Hsp60 was separately expressed in HEK293 cells. Then, total cellular protein was processed for immunoprecipitation (IP) with anti-14-3-3 protein antibody. The NTF but not CTF of Hsp60 was coimmunoprecipitated, indicating that the 14-3-3-interacting domain is located in the NTF of Hsp60 (Fig. 5A, panel a).

Phosphorylation-Independent Interaction of 14-3-3 Protein With Hsp60 and PrPC

By IP of human brain protein with anti-14-3-3 protein antibody, cellular prion protein (PrPC) along with Hsp60 was coimmunoprecipitated with 14-3-3 (Fig. 5B, panels a–c). In contrast, Raf-1, one of the well-known 14-3-3-binding partners, was not coimmunoprecipitated with 14-3-3 in the human brain homogenate (data not shown). By protein overlay of human brain homogenate, the rh14-3-3ζ probe reacted with PrPC, suggesting that PrPC is another 14-3-3 protein-interacting protein (Fig. 5C, panels a–c). Furthermore, the rh14-3-3ζ probe labeled both recombinant human Hsp60 (66 kDa) and PrPC (32 kDa), but did not label a LacZ fragment (44 kDa), all of which were produced by *E. coli* as non-phosphorylated forms tagged with Xpress (Fig. 5D, panels a–d). This indicates that the molecular interaction of 14-3-3 with Hsp60 and PrPC is direct but phosphorylation-independent. To identify the 14-3-3-binding site of PrPC, either the NTF (amino acid residues 23–137) or the CTF (amino acid residues 138–231) of human PrPC was separately expressed in HEK293 cells. Then, total cellular protein was processed

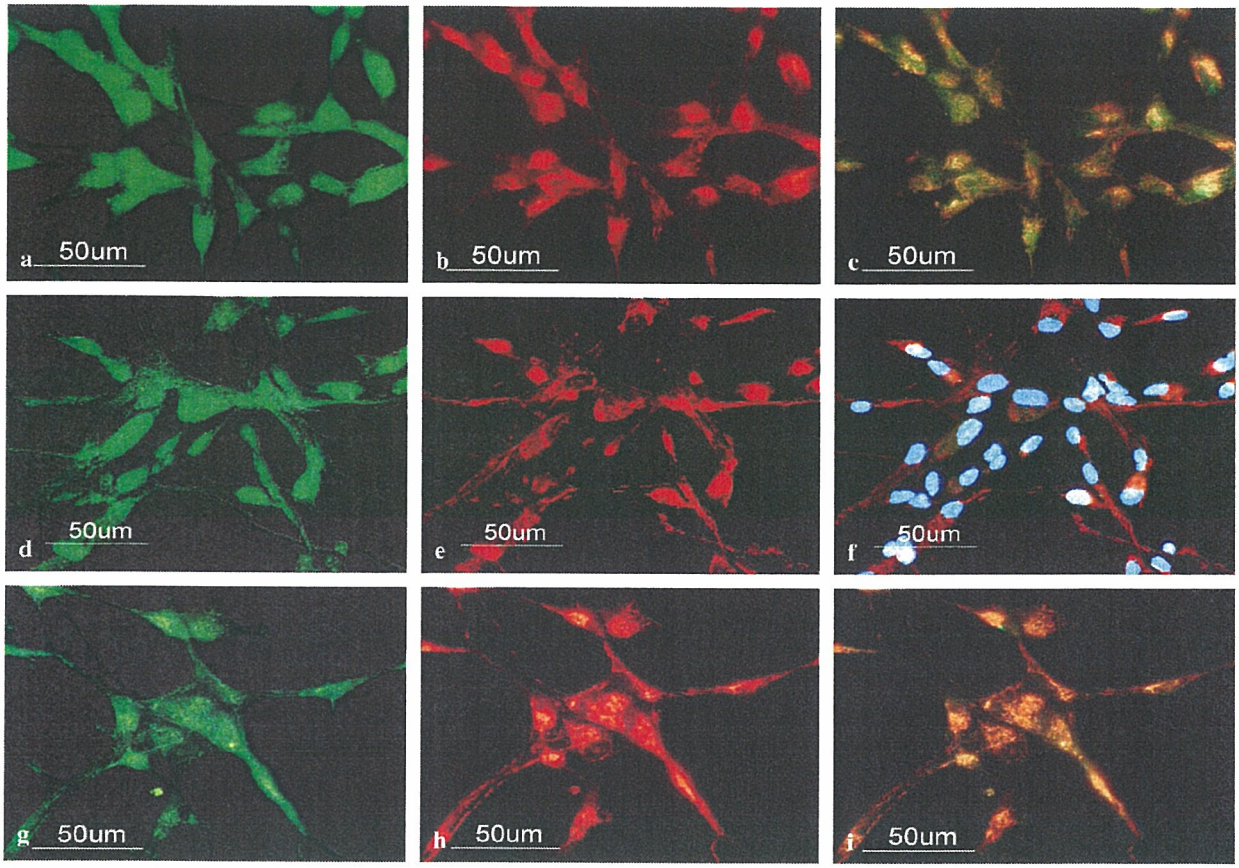

FIGURE 6. Colocalization of 14-3-3 protein, Hsp60, and PrPC in the mitochondria of human neuronal progenitor cells. Human neuronal progenitor (NP) cells were immunolabeled with 14-3-3ζ isoform-specific antibody, anti-Hsp60 antibody, anti-prion protein antibody (8G8), MitoTracker Red CMXRos, or DAPI followed by staining with secondary antibodies. **(a)** 14-3-3ζ, **(b)** Hsp60, **(c)** merge of **(a)** and **(b)**; **(d)** 14-3-3ζ, **(e)** CMXRos, **(f)** merge of **(d)** and **(e)** labeled with DAPI; **(g)** PrPC, **(h)** Hsp60, **(i)** merge of **(g)** and **(h)**.

for IP with anti-14-3-3 protein antibody. The NTF but not CTF of PrPC was coimmunoprecipitated, indicating that the 14-3-3-interacting domain is located in the NTF of PrPC (Fig. 5A, panel b).

Coexpression of 14-3-3 Protein, Hsp60, and PrPC in Vitro and in Vivo

To determine whether 14-3-3, Hsp60, and PrPC are colocalized in the same subcellular compartment, cultured human NP cells were double-immunolabeled with the 14-3-3ζ isoform-specific antibody, anti-Hsp60 antibody, and anti-prion protein antibody. An intense immunoreactivity for 14-3-3 was located chiefly in the cytoplasm, and less abundantly in the nucleus and the plasma membrane, whereas Hsp60 immunolabeling was found almost exclusively in the cytoplasm (Fig. 6a, b). Hsp60 showed a granular distribution pattern identical to the location of the mitochondria, where both 14-3-3 and Hsp60 were found to be colocalized (Fig. 6c). A considerable overlap was found between the 14-3-3 immunoreactivity and the staining of a mitochondrial dye, being devoid of the nucleus (Fig. 6d–f). Furthermore, PrPC was colocalized with Hsp60 (Fig. 6g–i). These results indicate that the 14-3-3 protein, Hsp60, and PrPC are colocalized chiefly in the mitochondria of human neuronal progenitor cells in culture, although an extramitochondrial coexpression of these proteins at very low levels could not be excluded.

In the human brain sections, nearly all of NSE^+ cortical neurons and $GFAP^+$ reactive astrocytes showed an intense cytoplasmic immunoreactivity for 14-3-3, Hsp60 and PrPC, suggesting that these three proteins are coexpressed most prominently in neurons (Fig. 7a–d) and reactive astrocytes (Fig. 8a–d) and to a lessor degree in microglia/macrophages (not shown) in the human CNS in vivo.

DISCUSSION

The present study, by protein overlay, mass spectrometry, and immunoprecipitation analysis, identified Hsp60 and PrPC as 14-3-3-interacting proteins. PrPC along with Hsp60 was coimmunoprecipitated with 14-3-3 from the human brain homogenate. The 14-3-3-binding domain is located in the NTF

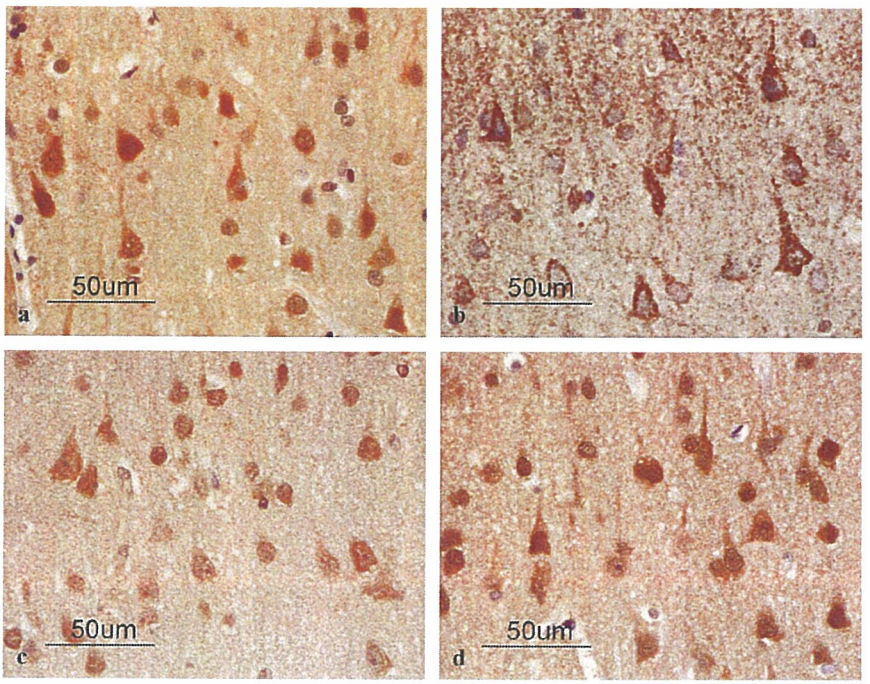

FIGURE 7. Coexpression of 14-3-3 protein, Hsp60, and PrPC in neurons in the human brain. Serial sections derived from autopsied brains of multiple sclerosis were processed for immunohistochemistry using 14-3-3ζ isoform-specific antibody, anti-Hsp60 antibody, anti-prion protein antibody (8G8), or anti-neuron-specific enolase (NSE) antibody. **(a–d)** The cerebral cortex of the frontal lobe of #791 MS: **(a)** 14-3-3ζ, **(b)** Hsp60, **(c)** PrPC, **(d)** NSE.

of Hsp60 and the NTF of PrPC in HEK293 cells overexpressing the transgenes. The 14-3-3 protein, Hsp60, and PrPC were colocalized chiefly in the mitochondria of human NP cells in culture, and they were coexpressed most obviously in neurons and reactive astrocytes in the human brain by immunohistochemistry. The interaction of 14-3-3 with Hsp60 and PrPC was phosphorylation-independent, because Hsp60 was found to be not substantially phosphorylated by the phosphoprotein gel stain, and the 14-3-3 probe reacted with nonphosphorylated forms of recombinant Hsp60 and PrPC by

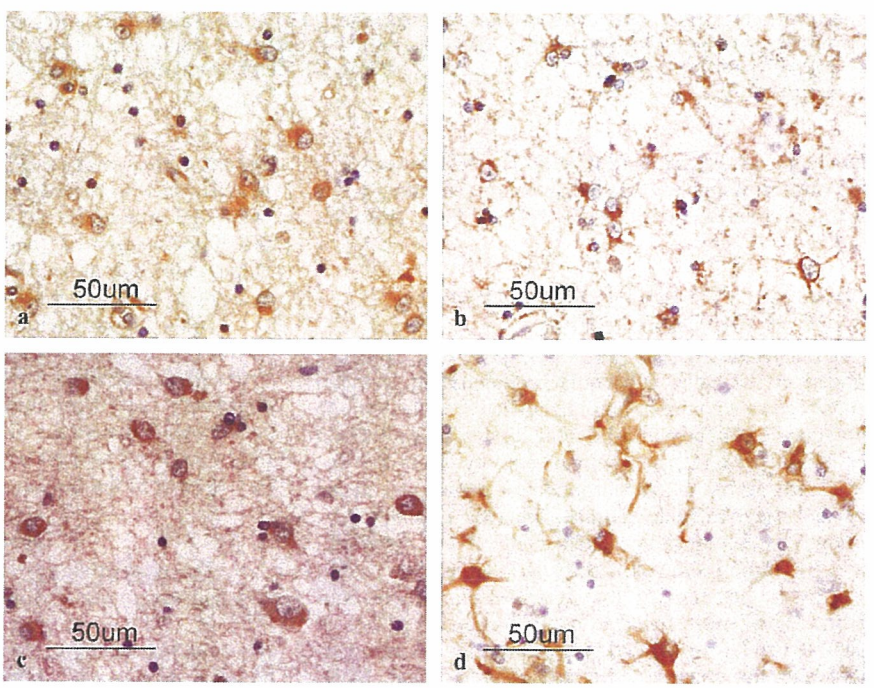

FIGURE 8. Coexpression of 14-3-3 protein, Hsp60, and PrPC in reactive astrocytes in the human brain. Serial sections derived from autopsied brains of multiple sclerosis were processed for immunohistochemistry using 14-3-3ζ isoform-specific antibody, anti-Hsp60 antibody, anti-prion protein antibody (8G8), or anti-GFAP antibody. **(a–d)** Chronic active demyelinating lesions in the subcortical white matter of the frontal lobe of 744 multiple sclerosis: **(a)** 14-3-3ζ, **(b)** Hsp60, **(c)** PrPC, **(d)** GFAP.

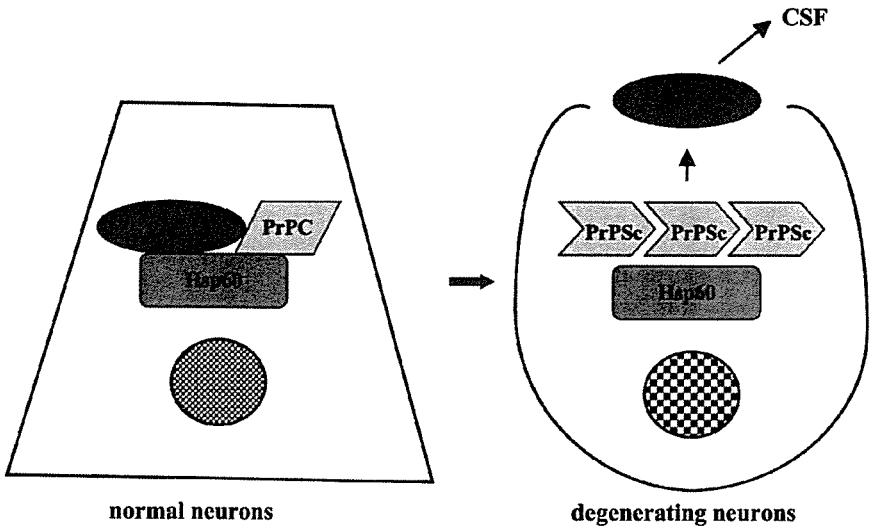

FIGURE 9. A possible mechanism for elevation of 14-3-3 protein in the cerebrospinal fluid of prion diseases. When affected with the pathogenetic prion, the molecular complex composed of 14-3-3, Hsp60, and PrPC becomes disintegrated during the conversion of PrPC into PrPSc aggregates, which displace the 14-3-3 protein from the complex, resulting in the release of 14-3-3 from degenerating neurons into the cerebrospinal fluid.

protein overlay analysis. These observations indicate that the 14-3-3 protein forms a molecular complex with Hsp60 and PrPC in the human CNS.

PrPC is a glycosylphosphatidylinositol (GPI) anchored cell-surface protein, expressed at highest levels in neurons and at substantial levels in astrocytes in the CNS (28, 29). Although a low level of extramitochondrial coexpression could not be excluded, the present study showed the substantial colocalization of 14-3-3, Hsp60, and PrPC in the mitochondria of human NP cells, not in agreement with the predominant location of PrPC on the cell surface. However, several recent studies showed that defined populations of neurons express PrPC in the cytoplasm as well as on the plasma membrane (27, 30). PrPC interacts with the C-terminus of Bcl-2 in the mitochondrial transmembrane region (31), and transgenic mice overexpressing wild-type PrPC show the expression of PrPC in the mitochondria (32), suggesting that the mitochondrial location of PrPC in cultured human NP cells does not seem unlikely. Increasing evidence suggests that the conformational conversion of α-helix-rich PrPC into β-sheet-rich PrPSc involves a molecular chaperone-like factor. A previous study using a yeast 2-hybrid system showed that Hsp60 interacts with PrPC, where the docking site was mapped between amino acid residues 180 and 210 of PrPC (33). GroEL, a homolog of eukaryotic Hsp60, mediates the aggregation of recombinant PrPC and promotes the conversion of PrPC into PrPSc in an ATP-dependent manner (23, 24). Furthermore, Hsp60 of the *Brucella abortus* directly binds PrPC of the host macrophages, and this binding promotes the aggregation of PrPC on the cell-surface lipid rafts (34). Interestingly, circulating antibodies against *Spiroplasma* Hsp60 were detected exclusively in patients with CJD, suggesting that the bacterial Hsp60, highly homologous to the host Hsp60, might play an active role in the pathologic process of prion diseases (35). Heat shock elements were identified in the promoter region of prion protein gene (36). PrPC exhibits an antioxidant activity (37), and stress-inducing stimuli such as reactive oxygen species, heat shock, and proinflammatory cytokines elevate the levels of PrPC expression in cultured cells (36, 38, 39). These observations suggest that PrPC and endogenous cellular Hsp are coordinately upregulated in certain cell types under pathologic conditions.

Supporting the present observations, several recent studies identified Hsp60 as one of 14-3-3-interacting proteins in HeLa and HEK293 cells by immunoaffinity purification (9, 40, 41). Hsp60 constitutes a heptameric cylindrical complex composed of identical subunits stacked back to back, forming a double-ring structure. The Anfinsen cage of Hsp60 contains a central cavity where substrate proteins are sequestered and properly folded in cooperation with the Hsp10 family protein (19, 20). In addition, several proteins that are too large to fit the cage are processed for chaperoning outside the cage (42). Hsp60 is located primarily in the mitochondrial matrix, where it mediates the folding of newly imported mitochondrial matrix proteins and the assembly of large multiprotein complexes (43). Importantly, the 14-3-3 protein that does not have a mitochondrial targeting signal is also identified within the mitochondria (44). A recent study showed that an exposure to cisplatin upregulates simultaneously Hsp60 and 14-3-3 expression in human squamous cell carcinoma (45). Kinase suppressor of Ras (KSR), a regulator of the Ras-MAP kinase pathway, forms a multimolecular signaling complex composed of Hsp90, Hsp70, Hsp68, $p50^{CDC37}$, MEK1, MEK2, and 14-3-3 proteins, where a panel of Hsp serve to stabilize KSR (46). It is worthy to note that the levels of expression of the cytosolic chaperonin CCT6A are reduced in the brain of 14-3-3γ isoform-knockout mice, although these mice show a clinical course similar to the wild-type mice after inoculation of scrapie prion (47). Because the 14-3-3 protein acts as an allosteric regulator that stabilizes the binding partners in a particular conformation (3, 4), we could suggest the following scenario (Fig. 9). The interaction of 14-3-3 with PrPC might prevent PrPC from the autocatalytic conformational change under physiological conditions. When affected with the pathogenetic prion, PrPSc aggregates displace 14-3-3

protein from the molecular complex during the conversion of PrPC into PrPSc that is promoted by Hsp60, resulting in the release of 14-3-3 from degenerating neurons into the CSF.

ACKNOWLEDGMENTS

The authors thank Dr. Masashi Fukuda, Invitrogen Proteome, Yokohama, Japan, for his help in nanoESI-MS/MS analysis; and Ms. Chizuru Soma and Ms. Ayako Sakamoto, NCNP, Tokyo, Japan, for their technical assistance. All autopsied brain samples were obtained from the Research Resource Network (RRN), Japan.

REFERENCES

1. Fu H, Subramanian RR, Masters SC. 14-3-3 proteins: Structure, function, and regulation. Annu Rev Pharmacol Toxicol 2000;40:617–47
2. van Hemert MJ, Steensma HY, van Heusden GPH. 14-3-3 proteins: Key regulators of cell division, signaling and apoptosis. Bioessays 2001; 23:936–47
3. Dougherty MK, Morrison DK. Unlocking the code of 14-3-3. J Cell Sci 2004;117:1875–84
4. MacKintosh C. Dynamic interactions between 14-3-3 proteins and phosphoproteins regulate diverse cellular processes. Biochem J 2004;381: 329–42
5. Berg D, Holzmann C, Riess O. 14-3-3 proteins in the nervous system. Nature Rev Neurosci 2002;4:752–62
6. Ostrerova N, Petrucelli L, Farrer M, et al. α-Synuclein shares physical and functional homology with 14-3-3 proteins. J Neurosci 1999;19:5782–91
7. Agarwal-Mawal A, Qureshi HY, Cafferty PW, et al. 14-3-3 connects glycogen synthase kinase-3β to tau within a brain microtubule-associated tau phosphorylation complex. J Biol Chem 2003;278:12722–28
8. Chen H-K, Fernandez-Funez P, Acevedo SF, et al. Interaction of Akt-phosphorylated ataxin-1 with 14-3-3 mediates neurodegeneration in spinocerebellar ataxia type 1. Cell 2003;113:457–68
9. Meek SEM, Lane WS, Piwnica-Worms H. Comprehensive proteomic analysis of interphase and mitotic 14-3-3-binding proteins. J Biol Chem 2004;279:32046–46
10. Zhai J, Lin H, Shamim M, et al. Identification of a novel interaction of 14-3-3 with p190RhoGEF. J Biol Chem 2001;276:41318–24
11. Henriksson ML, Francis MS, Peden A, et al. A nonphosphorylated 14-3-3 binding motif on exoenzyme S that is functional in vivo. Eur J Biochem 2002;269:4921–29
12. Dai J-G, Murakami K. Constitutively and autonomously active protein kinase C associated with 14-3-3 ζ in the rodent brain. J Neurochem 2003;84:23–34
13. Yuan H, Michelsen K, Schwappach B. 14-3-3 dimers probe the assembly status of multimeric membrane proteins. Curr Biol 2003;13:638–46
14. Hsich G, Kenney K, Gibbs CJ Jr., et al. The 14-3-3 brain protein in cerebrospinal fluid as a marker for transmissible spongiform encephalopathies. N Engl J Med 1996;335:924–30
15. Zerr I, Bodemer M, Gefeller O, et al. Detection of 14-3-3 protein in the cerebrospinal fluid supports the diagnosis of Creutzfeldt-Jakob disease. Ann Neurol 1998;43:32–40
16. Richard M, Biacabe A-G, Streichenberger N, et al. Immunohistochemical localization of 14.3.3 ζ protein in amyloid plaques in human spongiform encephalopathies. Acta Neuropathol 2003;105:296–302
17. Prusiner SB. Prions. Proc Natl Acad Sci U S A 1998;95:13363–83
18. Hartl FU, Mayer-Hartl M. Molecular chaperones in the cytosol: From nascent chain to folded protein. Science 2002;295:1852–58
19. Bukau B, Horwich AL. The Hsp70 and Hsp60 chaperone machines. Cell 1998;92:351–66
20. Richardson A, Landry SJ, Georgopoulos C. The ins and outs of a molecular chaperone machine. Trends Biochem Sci 1998;23:138–43
21. Muchowski PJ, Wacker JL. Modulation of neurodegeneration by molecular chaperones. Nature Rev Neurosci 2005;6:11–22
22. Hansen JJ, Dürr A, Cournu-Rebeix I, et al. Hereditary spastic paraplegia SPG13 is associated with a mutation in the gene encoding the mitochondrial chaperonin Hsp60. Am J Hum Genet 2002;70:1328–32
23. DebBurman SK, Raymond GJ, Caughey B, et al. Chaperone-supervised conversion of prion protein to its protease-resistant form. Proc Natl Acad Sci U S A 1997;94:13938–43
24. Stöckel J, Hartl FU. Chaperonin-mediated de novo generation of prion protein aggregates. J Mol Biol 2001;313:861–72
25. Satoh J-I, Kuroda Y. Differential gene expression between human neurons and neuronal progenitor cells in culture: An analysis of arrayed cDNA clones in NTera2 human embryonal carcinoma cell line as a model system. J Neurosci Methods 2000;94:155–64
26. Satoh J-I, Yamamura T, Arima K. The 14-3-3 protein ϵ isoform expressed in reactive astrocytes in demyelinating lesions of multiple sclerosis binds to vimentin and glial fibrillary acidic protein in cultured human astrocytes. Am J Pathol 2004;165:577–92
27. Kovacs GG, Voigtländer T, Hainfellner JA, et al. Distribution of intraneuronal immunoreactivity for the prion protein in human prion diseases. Acta Neuropathol 2002;104:320–26
28. Bendheim PE, Brown HR, Rudelli RD, et al. Nearly ubiquitous tissue distribution of the scrapie agent precursor protein. Neurology 1992;42: 149–56
29. Moser M, Colello RJ, Pott U, et al. Developmental expression of the prion protein gene in glial cells. Neuron 1995;14:509–17
30. Mironov A Jr, Latawiec D, Wille H, et al. Cytosolic prion protein in neurons. J Neurosci 2003;23:7183–93
31. Kurschner C, Morgan JI. Analysis of interaction sites in homo-and heteromeric complexes containing Bcl-2 family members and the cellular prion protein. Mol Brain Res 1996;37:249–58
32. Hachiya NS, Yamada M, Watanabe K, et al. Mitochondrial localization of cellular prion protein (PrP^C) invokes neuronal apoptosis in aged transgenic mice overexpressing PrP^C. Neurosci Lett 2005;374:98–103
33. Edenhofer F, Rieger R, Famulok M, et al. Prion protein PrP^C interacts with molecular chaperones of the Hsp60 family. J Virol 1996;70: 4724–28
34. Watarai M, Kim S, Erdenebaatar J, et al. Cellular prion protein promotes *Brucella* infection into macrophages. J Exp Med 2003;198:5–17
35. Moyer P. Spiroplasma Hsp60 may be the pathogen responsible for spreading CJD. Neurol Today 2004;4:8–11
36. Shyu W-C, Ham H-J, Saeki K, et al. Molecular modulation of expression of prion protein by heat shock. Mol Neurobiol 2002;26:1–12
37. White AR, Collins SJ, Maher F, et al. Prion protein-deficient neurons reveal lower glutathione reductase activity and increased susceptibility to hydrogen peroxide toxicity. Am J Pathol 1999;155:1723–30
38. Satoh J-I, Kurohara K, Yukitake M, et al. Constitutive and cytokine-inducible expression of prion protein gene in human neural cell lines. J Neuropathol Exp Neurol 1998;57:131–39
39. Sauer H, Dagdanova A, Hescheler J, et al. Redox-regulation of intrinsic prion expression in multicellular prostate tumor sheroids. Free Radic Biol Med 1999;27:1276–83
40. Jin J, Smith FD, Stark C, et al. Proteomic, functional, and domain-based analysis of in vivo 14-3-3 binding proteins involved in cytoskeletal regulation and cellular organization. Curr Biol 2004;14: 1436–50
41. Pozuelo Rubio M, Geraghty KM, Wong BHC, et al. 14-3-3-affinity purification of over 200 human phosphoproteins reveals new links to regulation of cellular metabolism, proliferation and trafficking. Biochem J 2004;379:395–408
42. Chaudhuri TK, Farr GW, Fenton WA, et al. GroEL/GroES-mediated folding of a protein too large to be encapsulated. Cell 2001;107:235–46
43. Cheng MY, Hartl FU, Martin J, et al. Mitochondrial heat-shock protein hsp60 is essential for assembly of proteins imported into yeast mitochondria. Nature 1989;337:620–25
44. Pierrat B, Ito M, Hinz W, et al. Uncoupling proteins 2 and 3 interact with members of the 14.3.3 family. Eur J Biochem 2000;267:2680–87
45. Castagna A, Antonioli P, Astner H, et al. A proteomic approach to cisplatin resistance in the cervix squamous cell carcinoma cell line A431. Proteomics 2004;4:3246–67
46. Stewart S, Sundaram M, Zhang Y, et al. Kinase suppressor of Ras forms a multiprotein signaling complex and modulates MEK localization. Mol Cell Biol 1999;19:5523–34
47. Steinacker P, Schwarz P, Reim K, et al. Unchanged survival rates of 14-3-3γ knockout mice after inoculation with pathological prion protein. Mol Cell Biol 2005;25:1339–46

International Immunology, Vol. 17, No. 12, pp. 1619–1629
doi:10.1093/intimm/dxh342

Preferential T_h2 polarization by OCH is supported by incompetent NKT cell induction of CD40L and following production of inflammatory cytokines by bystander cells *in vivo*

Shinji Oki, Chiharu Tomi, Takashi Yamamura and **Sachiko Miyake**

Department of Immunology, National Institute of Neuroscience, NCNP, 4-1-1 Ogawahigashi, Kodaira, Tokyo 187-8502, Japan

Keywords: cell activation, cytokines, inflammation, natural killer, rodent, T cells

Abstract

The altered glycolipid ligand OCH is a selective inducer of T_h2 cytokines from NKT cells and a potent therapeutic reagent for T_h1-mediated autoimmune diseases. Although we have previously shown the intrinsic molecular mechanism of preferential IL-4 production by OCH-stimulated NKT cells, little is known about the extrinsic regulatory network for IFN-γ production. Here we demonstrate that OCH induces lower production of IFN-γ, not only by NKT cells but also by NK cells compared with α-galactosylceramide. OCH induced lower IL-12 production due to ineffective primary IFN-γ and CD40 ligand expression by NKT cells, and resulted in lower secondary IFN-γ induction. Co-injection of a sub-optimal dose of IFN-γ and stimulatory anti-CD40 mAb compensates for the lower induction of IL-12 by OCH administration. IL-12 converts OCH-induced cytokine expression from IL-4 predominance to IFN-γ predominance. Furthermore, CpG oligodeoxynucleotide augmented IL-12 production when co-administrated with OCH, resulting in increased IFN-γ production. Taken together, the lower IL-12 production and subsequent lack of secondary IFN-γ burst support the effective T_h2 polarization of T cells by OCH. In addition, highlighted in this study is the characteristic property of OCH that can induce the differential production of IFN-γ or IL-4 according to the availability of IL-12.

Introduction

NKT cells are a unique subset of CD1d-restricted T lymphocytes that express TCR and some NKR. NKT cells recognize glycolipid antigens such as α-galactosylceramide (αGC) by an invariant TCRα chain composed of Vα14-Jα18 segments in mice and Vα24-Jα18 segments in humans, associated with TCRβ chains using a restricted set of Vβ genes (1, 2). NKT cells rapidly secrete large amounts of cytokines including IL-4 and IFN-γ upon antigen stimulation and are effective regulators of T_h1/T_h2 balance *in vivo* (3–5). We have previously demonstrated that *in vivo* administration to mice of altered glycolipid ligand, OCH, ameliorates experimental autoimmune encephalomyelitis (EAE), collagen-induced arthritis (CIA) and type I diabetes by enhancing IL-4-dependent T_h2 responses without inducing IFN-γ production and pathogenic T_h1 responses (6–8).

Recently, we have clarified the intrinsic molecular mechanism of preferential IL-4 production by OCH-stimulated NKT cells (9). IFN-γ production by NKT cells was more susceptible to the sphingosine length of glycolipid ligand than that of IL-4, and the length of sphingosine chain determined the half-life of NKT cell stimulation by CD1d-associated glycolipids. IFN-γ production by NKT cells required longer T cell stimulation than did IL-4 production and the transcription of the IFN-γ gene required *de novo* protein synthesis by activated NKT cells. The NF-κB family member transcription factor c-Rel was preferentially transcribed in αGC-stimulated, but not in OCH-stimulated, NKT cells and was identified as essential for IFN-γ production by activated NKT cells. Therefore, the differential duration of NKT cell stimulation, due to the binding stability of individual glycolipid antigens to CD1d molecules, determines whether signaling leads to effective c-Rel transcription and IFN-γ production by activated NKT cells.

Upon stimulation by αGC *in vivo*, NKT cells rapidly affect the functions of neighboring cell populations such as T cells, NK cells, B cells and dendritic cells (DCs) in a direct or indirect manner (10–13). The serial production of IFN-γ by NKT cells

Correspondence to: S. Miyake; E-mail: miyake@ncnp.go.jp

Transmitting editor: K. Okumura

Received 19 August 2005, *accepted* 30 September 2005

Advance Access publication 15 November 2005

and NK cells has been demonstrated, suggesting that activated NKT cells may influence further IFN-γ production by other cells including NK cells (3, 10). A C-glycoside analog of αGC has been shown to induce a superior T_h1-type response than αGC does by inducing higher IFN-γ production by NK cells. IL-12 was indispensable for the T_h1-skewing effect of the glycolipid, indicating the importance of IL-12 in enhanced IFN-γ production *in vivo* (14). Furthermore, αGC-stimulated NKT cells can act as an adjuvant *in vivo* by inducing the full maturation of DCs, as manifested by augmented co-stimulatory molecules and enhanced mixed leukocyte reactions (11). Accordingly, αGC-stimulated NKT cells were shown to express CD40 ligand (CD40L, CD154), which can engage CD40 on antigen-presenting cells and stimulate them to produce IL-12 (15, 16). Furthermore, IFN-γ production and T_h1-type responses were impaired in CD40-deficient mice (5). A growing body of evidence suggests that both extrinsic and intrinsic factors compose an intricate network for controlling IFN-γ production and T_h1 polarization after intensive stimulation of NKT cells by superagonistic glycolipid such as αGC.

Although the intrinsic molecular mechanism of preferential IL-4 production by OCH-stimulated NKT cells has been elucidated, little is known about the effect of OCH on bystander cells and the extrinsic regulatory network for IFN-γ production and T_h1 polarization. Considering the lower IFN-γ production by OCH compared with extensive IFN-γ production by αGC *in vivo*, OCH may affect the functions of neighboring cell populations in a different manner from that of αGC. In the current study, we demonstrate that OCH induces less effective production of IFN-γ and IL-12 by bystander cells possibly due to lower expression of CD40L by NKT cells. Co-administration of stimulatory anti-CD40 mAb in combination with IFN-γ enhanced the production of IL-12 induced by OCH *in vivo*, and IL-12 modulated OCH-induced cytokine expression by augmenting IFN-γ. Consistent with these results, co-administration of CpG oligodeoxynucleotide (ODN) with OCH preferentially induced IFN-γ production possibly through augmented IL-12 production. Considering that NKT cell responses to CD1d-presented self-antigens are modified by IL-12 to induce massive IFN-γ production during the course of microbial infection (17), OCH, at least partly, mimics the physiological behavior of the putative self-antigen for NKT cells in the context of cytokine milieu *in vivo*.

Methods

Reagents and antibodies

Murine IL-12, IFN-γ and Flt3-ligand (Flt3L) were purchased from Peprotech EC (London, UK). Anti-CD40 mAb (HM40-3) was purchased from BD Biosciences PharMingen (San Diego, CA, USA). Mouse anti-IFN-γ (R4-6A2) was purified from ascites of hybridoma obtained from American Type Culture Collection. Glycolipids were solubilized in dimethyl sulfoxide (100 μg ml^{-1}) and stored at −20°C until use. The following CpG ODN was synthesized: CpG ODN, 5′-GCATGACGTT-GAGCT-3′.

Mice

C57BL/6 (B6) mice were purchased from CLEA Laboratory Animal Corporation (Tokyo, Japan). MHC class II-deficient I-A^bβ−/− mice with the B6 background were purchased from Taconic (Germantown, NY, USA). All animals were kept under specific pathogen-free conditions and used at 7–12 weeks of age. Animal care and use were in accordance with institutional guidelines.

Induction of bone marrow-derived DCs

Bone marrow cells were isolated by flushing femurs of B6 mice and re-suspended in culture medium supplemented with murine Flt3L (100 ng ml^{-1}) as described in (18). Cells were harvested from the culture after 10 days and subjected to co-culture experiment with NKT cells.

Flow cytometry and intracellular cytokine staining

Spleen cells or liver mononuclear cells harvested after stimulation with glycolipids *in vivo* were cultured in complete media containing GolgiStop (BD PharMingen, San Jose, CA, USA). Then cells were incubated with Fc block (anti-mouse FcγIIIR/IIR mAb clone 2.4G2) and were stained with biotinylated anti-NK1.1 mAb (PK136), washed with PBS and then stained with peridinin chlorophyll protein/cyanine 5.5–anti-CD3 mAb and streptavidin–allophycoerythrin (APC). Then cells were washed twice with PBS and fixed in BD Cytofix/Cytoperm solution for 20 min at 4°C. After fixation, cells were washed with BD Perm/Wash solution and re-suspended in the same solution containing either PE–anti-IFN-γ mAb (XMG1.2) or PE-conjugated isotype control Ig for 30 min at 4°C. Then samples were washed and the stained cells were analyzed using a FACS Calibur instrument (Becton Dickinson) with CELLQuest software (Becton Dickinson). Identification of iNKT cells by Dimer XI Recombinant Soluble Dimeric Mouse CD1d (BD PharMingen) was performed as described previously (19). For analysis of CD40L expression, spleen cells harvested after stimulation with glycolipids *in vivo* for indicated periods of time were cultured in complete media containing biotinylated anti-CD40L mAb (MR1) for 2 h. Cells were harvested, washed with PBS and stained with FITC–anti-CD3 mAb, PE–anti-NK1.1 mAb and streptavidin–APC for 20 min. CD40L expression was analyzed in CD3/NK1.1 double-positive cell.

Microarray

Microarray analysis was performed as described previously (9). In brief, I-A^bβ−/− mice pre-treated with anti-asialo GM_1 antibody were injected with αGC or OCH (100 μg kg^{-1}). Total RNA was isolated from liver NKT cells (purified as CD3+ NK1.1+ cells) and applied to microarray by using U74Av2 arrays (GeneChip System, Affymetrix, Santa Clara, CA, USA). From data image files, gene transcript levels were determined using algorithms in the GeneChip Analysis Suit software (Affymetrix).

Quantitative reverse transcription–PCR

Quantitative reverse transcription–PCR was conducted using a Light Cycler-FastStart DNA Master SYBR Green I kit (Roche Molecular Biochemicals) as described previously (9). Primers used for the analysis of gene expression are as follows; CD40L (F) CGAGTCAACGCCCATTCATC, (R) GTAATTCAAA-CACTCCGCCC.

ELISA

The level of cytokine production in cell culture supernatants or in serum was evaluated by standard sandwich ELISA, employing purified and biotinylated mAb sets (11B11/BVD6-24G2 for IL-4, R4-6A2/XMG1.2 for IFN-γ and 9A5/C17.8 for IL-12) and standards (OptEIA set, BD PharMingen) as described previously (9). After adding a substrate, the reaction was evaluated using a Microplate reader (BioRad).

Statistics

For statistic analysis, non-parametric Mann–Whitney test was used to calculate significance levels for all measurements. Values of $P < 0.05$ was considered statistically significant.

Results

OCH induces lower IFN-γ expression than αGC in both NKT cells and NK cells in vivo

Although NKT cells are a major source of IL-4 after glycolipid administration *in vivo*, activated NKT cells are shown to affect the functions of bystander cells such as T cells, NK cells, B cells and DCs in a direct or indirect manner, resulting in possible secondary augmentation of IFN-γ production by these cells. To evaluate the contribution of NKT cells and other cells for IFN-γ production after glycolipid administration, we performed kinetic analysis of cytokine production by splenic NKT cells, NK cells, T cells and other cells after *in vivo* administration of glycolipids. IFN-γ production was detected both in NKT cells and NK cells (Fig. 1A), and neither CD3+ T cells nor CD3−NK1.1− cells showed significant IFN-γ production 2 or 6 h after glycolipid administration. αGC induced a larger population of IFN-γ-producing NKT cells than OCH did which is consistent with the previous report (9). The kinetic analysis revealed that IFN-γ production by NKT cells was dominant in earlier time points (2 h) after glycolipid administration and IFN-γ production by NK cells was comparable or even higher at later time points (6 h) (Fig. 1B), suggesting that IFN-γ production by NKT cells preceded IFN-γ production by NK cells as reported previously (3, 10). As CD3+NK1.1+ cells do not always represent CD1d-restricted iNKT cells, we compared IFN-γ production by CD1d-dimerX-positive T cells after treatment with αGC or OCH. Again, αGC induced a larger population of IFN-γ-producing iNKT cells than OCH did (Fig. 1C). Interestingly, αGC induced a much larger population of IFN-γ-producing NK cells than

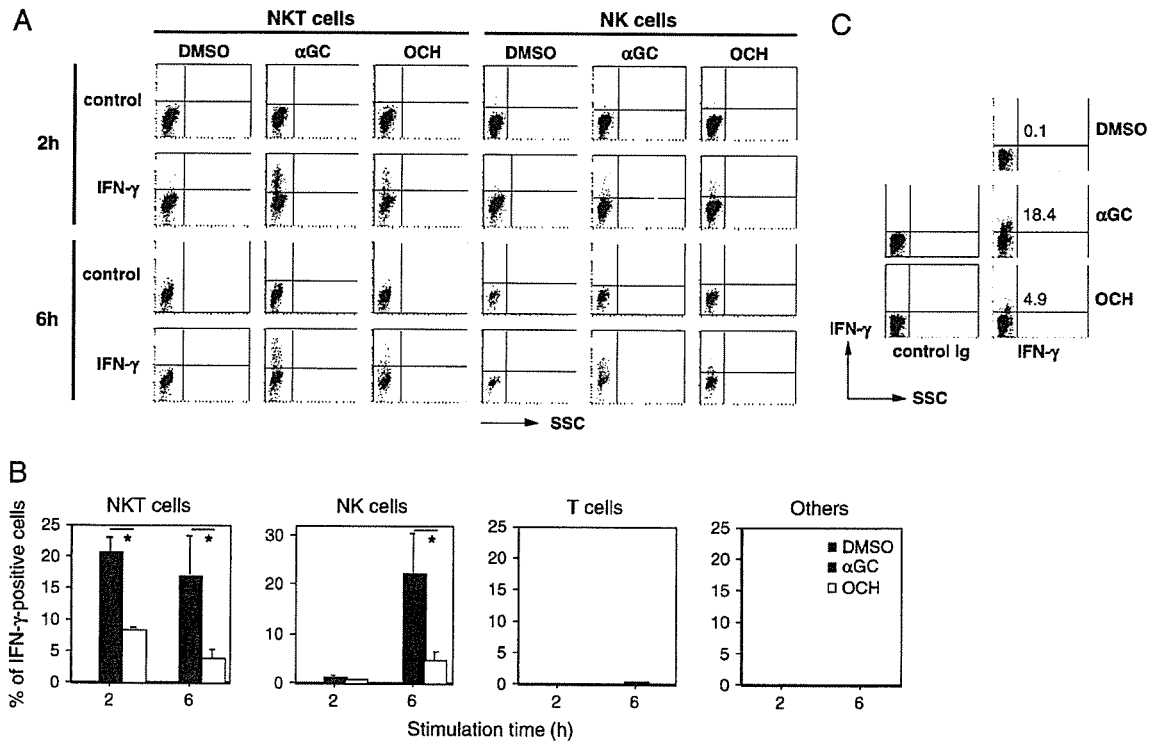

Fig. 1. Expression of IFN-γ by NKT cells and non-NKT cells after administration of glycolipid ligands. B6 mice were treated intra-peritoneally with 2 μg per mouse of either αGC or OCH, and spleen cells were harvested at various time points after glycolipid administration and subjected to intracellular cytokine staining as described in Methods. (A) Data analyzed for CD3+NK1.1+ NKT cells, CD3−NK1.1+ NK cells, CD3+NK1.1− T cells and CD3−NK1.1− cells were shown for the presence of intracellular IFN-γ. Similar results were obtained by analyzing liver mononuclear cells after glycolipid administration (data not shown). (B) Plotted values represent the percentage of IFN-γ-positive cells (mean ± SD for triplicate samples) in the gated population after treatment with dimethyl sulfoxide (DMSO) (hatched bar), αGC (filled bar), or OCH (open bar). (C) Data analyzed for CD1d-DimerX-positive iNKT cells were shown for the presence of intracellular IFN-γ 2 h after glycolipid treatment. The experiments shown are representative of three independent experiments. *$P < 0.05$.

OCH, suggesting that OCH induces less IFN-γ production than αGC not only by direct effect on NKT cells but also by indirect effect on NK cells. To exclude the possibility of the contamination of activated non-CD1d-restricted T cells into NKT fractions or activated NKT cells into NK cells fraction due to the down-regulation of TCR, we conducted the following experiments. First, αGC-loaded DimerXI-stained cells were concentrated in the NK1.1+CD3+ population and <0.4% of cells were reactive to αGC-loaded DimerXI either in NK1.1+CD3− or NK1.1−CD3+ cell populations. Second, >95% of αGC-loaded DimerXI-reactive spleen cells were positive for both CD3 and NK1.1 after stimulation with glycolipids. Third, most of the intracellular IFN-γ-positive CD3− cells were DX5 positive 2 and 6 h after stimulation with glycolipids (data not shown). These results indicated that the contamination of IFN-γ-producing cells into the other fractions was minimum.

αGC-induced IFN-γ production by NK cells is partly dependent on IFN-γ produced by NKT cells

To determine the effect of IFN-γ on consequent IFN-γ production by NK cells, we treated mice with anti-IFN-γ mAb before administration of αGC, and then examined IFN-γ-producing cells using intracellular staining. As shown in Fig. 2, there was no significant difference in the frequency of IFN-γ-producing NKT cells after administration of αGC with or without anti-IFN-γ mAb. Meanwhile, co-administration of anti-IFN-γ mAb showed ~35% reduction in IFN-γ-producing NK cells after αGC treatment (Fig. 2, right panel). These results suggested that NKT cell-derived IFN-γ was involved in αGC-induced IFN-γ production by NK cells to some extent, but an IFN-γ-independent mechanism might be involved in indirect up-regulation of IFN-γ production by NK cells after αGC administration *in vivo*.

OCH administration does not induce effective IL-12 production

As DCs were demonstrated to be activated after *in vivo* administration of αGC (11, 20) to produce large amount of IL-12 (21) and IL-12 is one of the most potent inducers of IFN-γ (22), we performed kinetic cytokine analysis of serum levels of IL-12 (p70) together with IFN-γ and IL-4 after intraperitoneal injection of the glycolipids into B6 mice. As shown in Fig. 3, administration of αGC induced a rapid elevation of IL-4 and a delayed elevation of IFN-γ in B6 mice. In contrast, administration of OCH induced a rapid elevation of IL-4 comparable to that induced by αGC with significantly less amount of elevation of IFN-γ, resulted in T_h2 skewing as described previously. Although the level of IL-12 in serum was observed 6 h after αGC injection, OCH injection induced one-tenth amount of serum IL-12 level compared with αGC. In addition, freshly isolated liver NKT cells co-cultured with Flt3L-induced DCs produced significantly higher amount of IL-12 in the presence of αGC compared with OCH. Meanwhile, Flt3L-induced DCs loaded with either αGC or OCH exerted comparable amount of IL-4 production (Fig. 3B), demonstrating directly that DCs loaded with OCH produce less IL-12 upon co-culture with NKT cells than DCs loaded with αGC, and therefore suggest that the *in vivo* effects of OCH are not simply due to its preferential presentation by antigen-presenting cells that produce less IL-12. Taken together, these results indicated that OCH administration did not induce effective IL-12 production *in vivo*.

Lower expression of CD40L on OCH-stimulated NKT cells

Activated NKT cells stimulate DCs to produce IL-12 through the engagement of CD40 on DCs with CD40L inducibly expressed on NKT cells (15, 21). Furthermore, a C-glycoside analog of αGC induced a superior IFN-γ production by NK cells than αGC does in an IL-12-dependent manner (14),

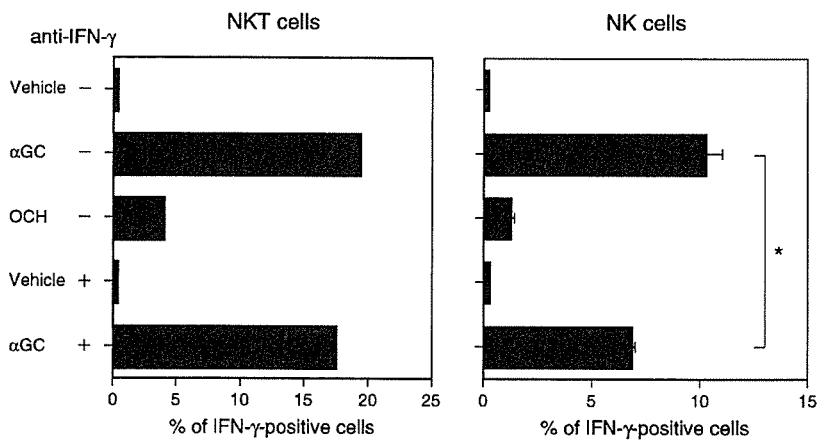

Fig. 2. αGC-induced IFN-γ production by NK cells is partly dependent on IFN-γ production by NKT cells. B6 mice were treated intra-peritoneally with 2 μg per mouse of glycolipids with or without 500 μg per mouse of anti-IFN-γ mAb. Four hours after treatment, spleen cells were harvested and subjected to intracellular cytokine staining. Plotted values represent the percentage of IFN-γ-positive cells (mean ± SD for triplicate samples) in the gated population for CD3+NK1.1+ NKT cells (left) or CD3−NK1.1+ NK cells (right). Similar results were obtained by analyzing liver mononuclear cells after glycolipid administration (data not shown). The experiments shown are representative of three independent experiments. *$P < 0.05$.

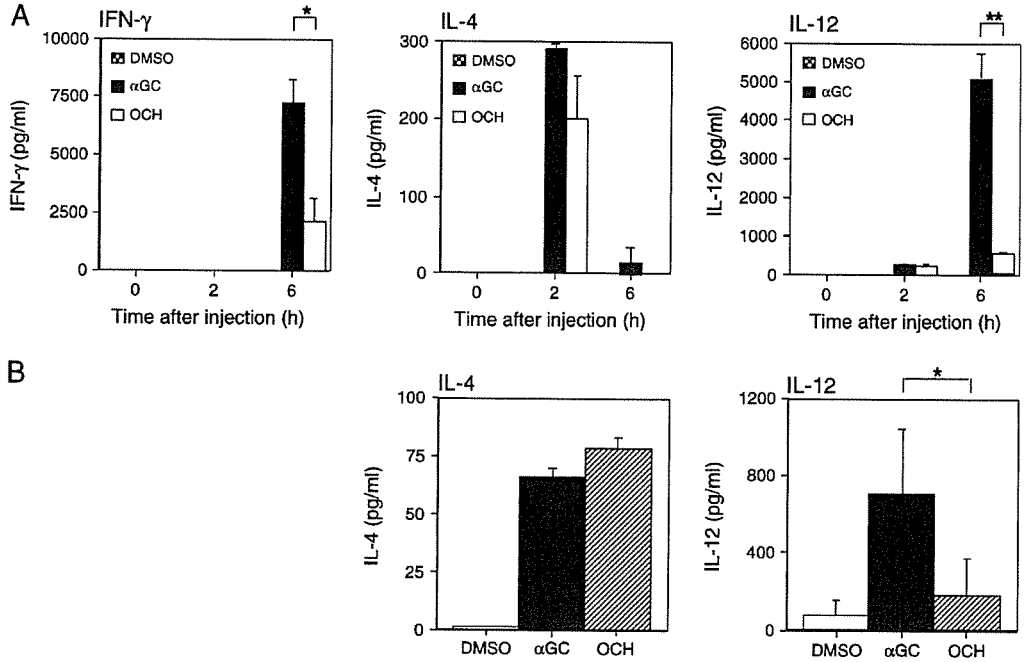

Fig. 3. OCH administration does not induce effective IL-12 production. (A) B6 mice were injected intra-peritoneally with vehicle alone, 2 μg per mouse of αGC or OCH and serum samples were collected at indicated times after injection. Serum levels of IFN-γ, IL-4 and IL-12 (mean ± SD) were determined by ELISA. This figure represents one of two experiments with similar results. $*P < 0.05$, $**P < 0.01$. (B) Freshly isolated liver NKT cells were co-cultured with Flt3L-induced DCs in the presence of αGC or OCH for 72 h. Levels of IL-4 and IL-12 were determined by ELISA. Data are expressed as mean ± SD for triplicate wells and representative data of two similar experiments are shown. $*P < 0.05$.

which suggests that IFN-γ production by NK cells might be regulated by IL-12. To clarify the mechanisms of lack of IL-12 production upon stimulation with OCH, we compared the inducible expression of CD40L on NKT cells after *in vivo* administration of glycolipids. Microarray analysis revealed that CD40L transcripts were inducibly expressed in NKT cells 1.5 h after stimulation with αGC and disappeared 12 h after stimulation. In contrast, OCH treatment induced approximately one-third of CD40L transcription compared with the effect of αGC (Fig. 4A). Consistent with the data of microarray analysis, real-time PCR analysis confirmed the preferential up-regulation of CD40L transcript after αGC stimulation (Fig. 4B). To demonstrate the differential expression of CD40L between αGC-stimulated and OCH-stimulated NKT cells, surface expression of CD40L on NKT cells were compared by flow cytometry after *in vivo* treatment with the glycolipids. As shown in Fig. 4(C), αGC induced higher expression of CD40L than OCH did on the surface of NKT cells. If compared quantitatively by mean fluorescence intensity of CD40L-positive subsets after treatment with either glycolipid, OCH treatment induced less CD40L expression on NKT cells compared with the effect of αGC (Fig. 4C, right panel). These results indicated that CD40L expression on αGC-stimulated NKT cells was significantly higher than that on OCH-stimulated NKT cells.

Co-administration of IFN-γ and CD40 stimulation augments IL-12 production by OCH in vivo

Although the CD40 pathway plays an intrinsic role in physiological conditions in eliciting IL-12 production, effective production of bioactive IL-12 by DCs requires another signal mediated by innate signals such as microbial stimuli (23) or by IFN-γ (24–26). Therefore, OCH-induced expression of CD40L and IFN-γ may not be effective to initiate IL-12 production from DCs *in vivo*. To test this hypothesis, we examined whether co-administration of stimulatory anti-CD40 mAb and/or IFN-γ confer OCH to induce higher IL-12 production. As shown in Fig. 5, administration of IFN-γ, stimulatory anti-CD40 mAb or combination of both reagents did not induce IL-12 expression *in vivo*. On the contrary, OCH-induced IL-12 production was partially augmented by co-administration of anti-CD40 mAb. Furthermore, concomitant administration of IFN-γ and stimulatory anti-CD40 mAb with OCH induced IL-12 production. These results suggest that the signals through CD40 and IFN-γ provided by OCH-stimulated NKT cells did not lead to efficient production of IL-12.

Co-administration of IL-12 augments IFN-γ production by OCH in vivo

A series of experiments so far indicated that OCH was less effective for induction of CD40L, IFN-γ and consequent IL-12 production than those induced by αGC. To examine directly the role of IL-12 production in less effective IFN-γ production by NKT cells and NK cells after OCH administration, we tested whether co-administration of IL-12 with OCH induces IFN-γ *in vitro* and *in vivo*. As shown in Fig. 6(A), IL-12 augmented IFN-γ production from spleen cells after *in vitro* treatment with

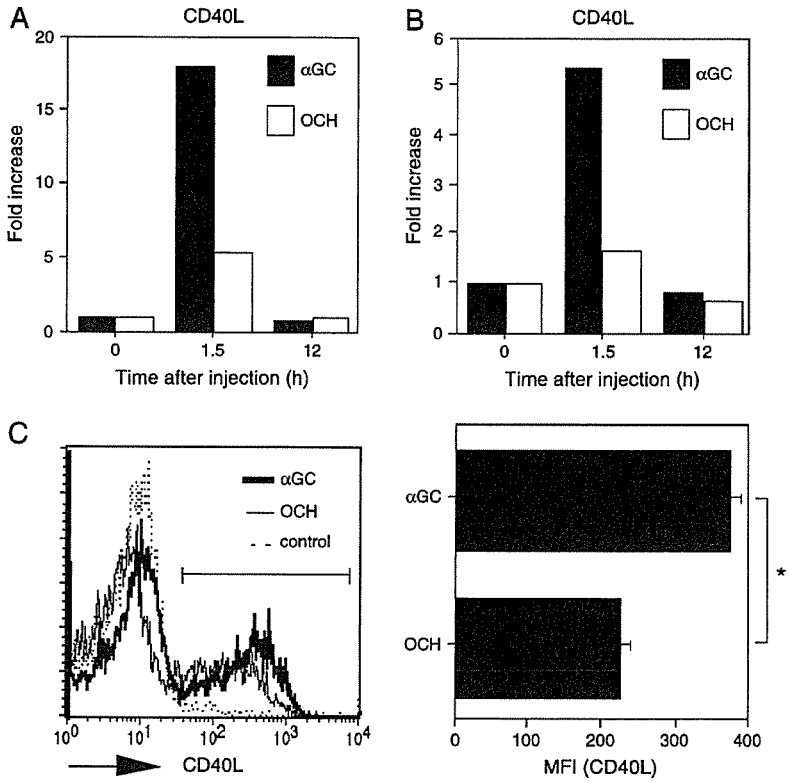

Fig. 4. Expression of CD40L on NKT cells stimulated with αGC or OCH. (A) Plotted values represent data of Affymetrix microarray analysis for indicated genes. The αGC- or OCH-stimulated liver NKT cells (purified as CD3+ NK1.1+ cells) as well as unstimulated NKT cells were analyzed at the indicated time points and the data represent to the relative values for glycolipid-treated samples when the value in NKT cells derived from untreated animals was defined as 1. (B) Real-time PCR analysis for the expression of CD40L mRNA. Data are presented as a fold induction of cytokine mRNAs after glycolipid treatment. The amount of mRNA in NKT cells derived from untreated animals was defined as 1. (C) Cell-surface expression of CD40L on αGC-stimulated (bold line) or OCH-stimulated (thin line) NKT cells. CD40L expression was analyzed in CD3/NK1.1 double-positive cell. Dotted line represents the histogram of control staining. B6 mice were injected intra-peritoneally with either αGC or OCH and liver mononuclear cells were isolated at the indicated time point. Cell-surface expression of CD40L was analyzed by flow cytometry (left) and plotted (right) as mean fluorescence intensity (MFI). Data are expressed as mean ± SD for duplicate samples. This figure represents one of two experiments with similar results. $*P < 0.05$.

OCH in a dose-dependent manner. Higher doses of IL-12 induced IFN-γ production even without OCH and the effect of OCH is concealed in this condition. Interestingly, IL-12 treatment inhibits IL-4 production by OCH-stimulated spleen cells in a dose-dependent manner, suggesting the reciprocal regulation of cytokine production by IL-12. Next we examined the effect of co-administration of sub-optimal dose of IL-12 together with OCH. As shown in Fig. 6(B), co-administration of OCH and IL-12 induced significantly higher production of IFN-γ compared with either treatment alone, although sub-optimal dose of IL-12 alone failed to induce IFN-γ production. In contrast, co-administration of IL-12 did not enhance the IL-4 production 2 h after OCH administration *in vivo*. As both NKT cells and NK cells are important sources of IFN-γ after glycolipid stimulation, we evaluated the frequency of IFN-γ-producing NKT and NK cells after co-administration of OCH with IL-12. As shown in Fig. 6(C), IL-12 augmented the proportions of IFN-γ-producing cells in both cell populations, but not in conventional T cells, when co-administered with OCH. These results demonstrated that the properties of OCH for less effective IFN-γ production by NKT cells and NK cells could be compensated by co-administration of IL-12.

Modification of cytokine profiles by pathogen-associated molecular patterns after OCH treatment in vivo

As sub-optimal dose of IL-12 was able to rescue defective IFN-γ production by administration of OCH alone, availability of IL-12 might be a crucial determinant for OCH-induced production of IFN-γ. As DCs and phagocytes produce IL-12 in response to pathogens during infection, pathogen-associated molecular patterns (PAMPs) are possible important determinants for cytokine profiles after OCH stimulation *in vivo*. We applied CpG ODN (27), which skews the host's immune milieu in favor of T_h1 responses by enhancing the production of pro-inflammatory cytokines including IL-12 (28), for analyzing cytokine profile of OCH. As shown in Fig. 7(A), CpG ODN alone induced no cytokine production within 6 h after injection. Concomitant injection of CpG ODN with OCH induced strong IFN-γ production (7.5-fold induction with 10 μg per mouse of CpG ODN plus OCH and 14-fold induction with 100 μg per

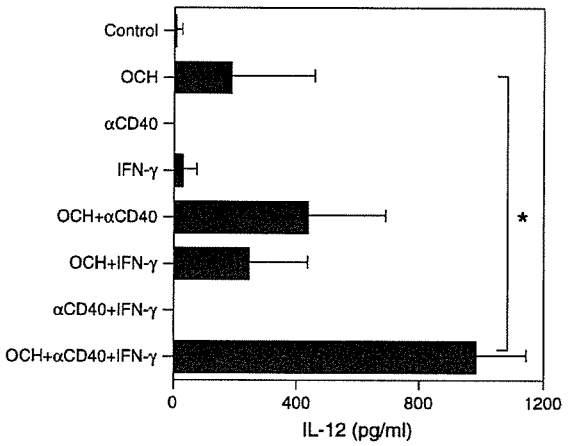

Fig. 5. Co-administration of IFN-γ and stimulatory anti-CD40 mAb augments IL-12 production after OCH administration *in vivo*. B6 mice were treated intra-peritoneally with 2 μg per mouse of glycolipids in combination with murine IFN-γ (1 μg per mouse) and/or stimulatory anti-CD40 mAb (100 μg per mouse) and serum samples were collected 2 h after treatment. The level of IL-12 production was determined by ELISA. These data represent one of two experiments with similar results. $*P < 0.05$.

mouse of CpG ODN plus OCH) and induced moderate IL-4 production (2.6-fold induction with 10 μg per mouse of CpG ODN plus OCH and 2.1-fold induction with 100 μg per mouse of CpG ODN plus OCH). Accordingly, co-administration of OCH and 10 μg per mouse of CpG ODN exhibited strong induction of IL-12 production (Fig. 7B, left panel), suggesting the synergic effect of OCH and CpG ODN for preferential up-regulation of IL-12. These results suggested that the PAMPs could be a considerable determinant for the cytokine profile following *in vivo* administration of OCH through regulating the availability of pro-inflammatory cytokines such as IL-12.

Discussion

In this study, we clarified the effect of OCH on bystander cell activation including the sequential IFN-γ production by NK cells and the functional conditioning of DCs. *In vivo* administration of OCH induced much lower IFN-γ production from both NKT and NK cells compared with that induced by αGC administration. NKT cell-derived IFN-γ was partially involved in inducing IFN-γ production by NK cells after αGC administration, implying that an IFN-γ-independent mechanism is also important for indirect up-regulation of IFN-γ production by NK cells after αGC administration *in vivo*. OCH administration induced lower CD40L expression by NKT cells compared with αGC administration, resulting in the lower production of IL-12 by DCs. Co-injection of stimulatory CD40 mAb and IFN-γ with OCH augmented the OCH-induced IL-12 production. Likewise, co-injection of IL-12 with OCH enhanced the production of IFN-γ by OCH administration alone. Furthermore, administration of OCH and CpG ODN into mice selectively induced IFN-γ production *in vivo*.

Consistent with the previous reports (9, 29), we here demonstrated that OCH administration induced less amount of IFN-γ than that of αGC in iNKT cells. Supporting these observation is another report in which truncation of the phytosphingosine lipid chain of αGC increases the relative amounts of IL-4 release by human NKT cells (30).

The functional relevance between NKT cells and NK cells was demonstrated in which NK-sensitive tumor incidence was higher and the time of tumor development was earlier in NKT cell-deficient mice compared with B6 mice (31). Considering that NKT cell-deficient mice still possess NK cells (32), NKT cells might serve as a modulator of NK cell function in tumor immunity, though the molecular mechanisms of how NKT cells modulate NK cells has not been clarified yet. Recently, β-anomeric galactosylceramide has been reported to have a capacity to reduce numbers of NKT cells without inducing typical NK cell-mediated responses (29, 33). We demonstrated in this study that OCH-induced IFN-γ production by NK cells was lower compared with that induced by αGC. This is at least partly due to the lower induction of IFN-γ by OCH-stimulated NKT cells and the lower induction of IL-12 by DCs, leading to weak activation of NK cells. There is a report showing that OCH and αGC can induce comparable amount of IFN-γ by NK cells 8 and 24 h after stimulation (29), even though serum levels of IFN-γ induced by OCH treatment were significantly lower than that by αGC treatment 6 or 24 h after stimulation. Since the major producer of IFN-γ *in vivo* after treatment with glycolipids at the later time points were demonstrated to be NK cells (3, 10), it is not clear whether cells other than NKT cells or NK cells could be the IFN-γ producer after αGC stimulation in their experimental condition. Although the basis for the discrepancy is not clear, it may be related to the difference in the synthetic methods of those glycolipids. Nevertheless, we reproducibly confirmed the *in vivo* ameliorating effects of OCH in various autoimmune mouse models including EAE, CIA and inflammatory bowel disease (7, 8, 34) through the differential induction of various cytokines.

The CD40 pathway plays an intrinsic role in physiological conditions by eliciting IL-12 production by DCs (35, 36). However, cross-linking of CD40 alone has been shown to be incapable of inducing IL-12 production by DCs. Schulz *et al.* (23) has demonstrated that effective production of bioactive IL-12 by DCs through T cell activation should be initiated by innate signals such as microbial stimuli. Activated T cell-mediated IL-12 production by DCs through CD40 signaling requires another signal, for example, IFN-γ (24–26), which is also shown to be required for uncommitted immature DCs to develop the capacity to produce high levels of IL-12 upon subsequent contact with naive T cells (25). Consistent with the observation, IFN-γ enhances gene transcription encoding both the p40 and p35 components of IL-12, resulting in a particularly marked production of the heterodimeric IL-12 (37, 38). Intriguingly, αGC-induced expression of IL-12R on NKT cells requires the production of IFN-γ by NKT cells and the production of IL-12 by DCs (21). In addition, IL-12 itself has been shown to act directly on DCs to promote IL-12 production (39). αGC provides dual signals to DCs by up-regulating CD40L on NKT cells and by inducing IFN-γ production by NKT cells, resulting in a large amount of IL-12 production by DCs. Our reconstitution experiment clearly showed that signals through CD40 and IFN-γ provided by OCH lead to small

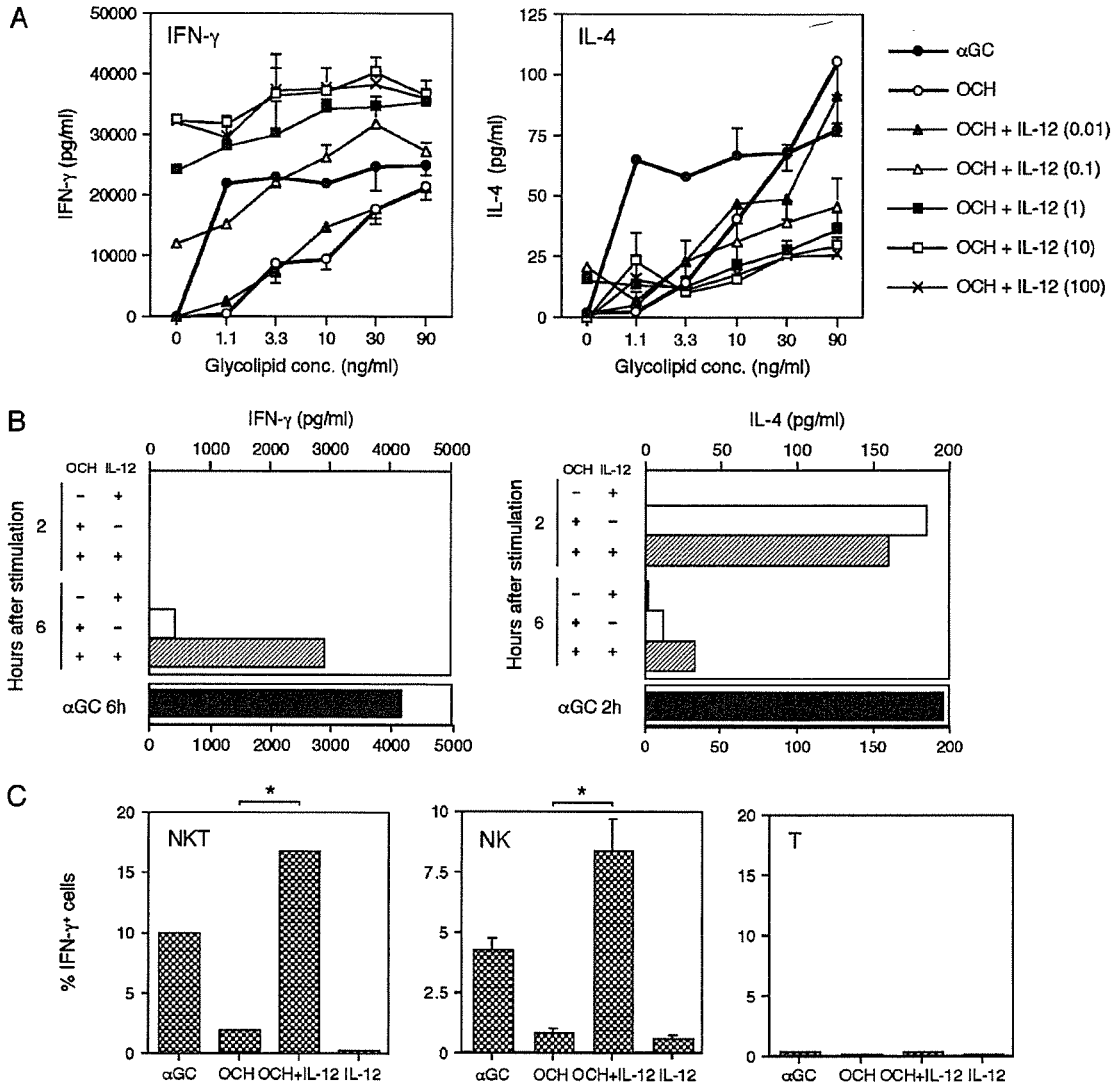

Fig. 6. Co-administration of IL-12 augments IFN-γ production by OCH. (A) Effects of IL-12 on cytokine production of splenocytes stimulated with glycolipids *in vitro*. Splenocytes were stimulated with various concentration of αGC or OCH in the presence or absence of IL-12 (with concentrations from 0.01 to 100 ng ml $^{-1}$) for 72 h and the levels of IFN-γ (left) or IL-4 (right) in the supernatants were measured by ELISA. Data are expressed as mean ± SD for triplicate wells. This figure represents one of two experiments with similar results. (B) Effects of IL-12 on cytokine production after glycolipid administration *in vivo*. B6 mice were treated with 10 ng per mouse of IL-12, 2 μg per mouse of OCH or OCH plus IL-12 and serum samples were collected at indicated times after injection. Serum levels of IFN-γ (left) and IL-4 (right) were determined by ELISA. This figure represents one of three experiments with similar results. (C) B6 mice were treated with 100 ng per mouse of IL-12 alone or in combination with 2 μg per mouse of OCH and spleen cells were harvested at various time points after glycolipid administration and subjected to intracellular cytokine staining as described in Methods. NKT cells, NK cells and T cells were analyzed for the presence of intracellular IFN-γ as described in Fig. 1. Similar results were obtained by analyzing liver mononuclear cells after glycolipid administration (data not shown). Data are expressed as mean ± SD for triplicate wells and represent one of two experiments with similar results. *$P < 0.05$.

amount of IL-12 production from DCs that is unable to trigger the IFN-γ burst by NKT cells and NK cells.

Treatment of mice with OCH together with sub-optimal doses of IL-12 resulted in significantly augmented IFN-γ production *in vivo*, indicating that the impaired IL-12 production by OCH is likely to be one of the major causes for less effective IFN-γ production *in vivo*. Similar observations were reported previously, in which treatment of mice with sub-optimal doses of αGC together with sub-optimal doses of IL-12 resulted in strongly enhanced natural killing activity and IFN-γ production (21). These results indicate an important role for DC-derived IL-12 for glycolipid-induced activation of NKT cells and suggest that NKT cells may be able to condition DCs for subsequent immune responses. To further clarify the

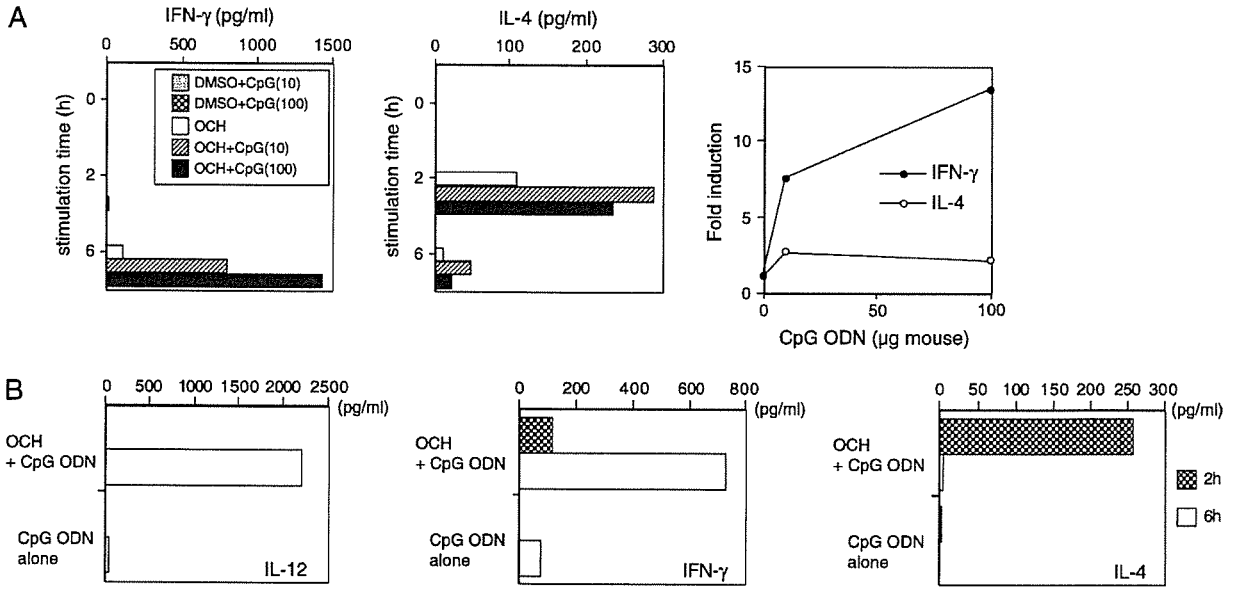

Fig. 7. Co-administration of CpG ODN augments IFN-γ production by OCH stimulation *in vivo*. (A) B6 mice were injected with 10 μg per mouse or 100 μg per mouse of CpG ODN alone or in combination with 2 μg per mouse of OCH and serum samples were collected at indicated times after injection. Serum levels of IFN-γ (left) or IL-4 (center) were determined by ELISA. The ratio of cytokine production was plotted in the right panel as fold induction for IFN-γ (at 6 h after injection) and IL-4 (at 2 h after injection). This figure represents one of two experiments with similar results. (B) B6 mice were injected with 10 μg per mouse of CpG ODN alone or in combination with 2 μg per mouse of OCH and serum samples were collected at indicated times after injection. Serum levels of IL-12 (left), IFN-γ (center) or IL-4 (right) were determined by ELISA. This figure represents one of three experiments with similar results.

cooperative roles of IL-12 for effective IFN-γ production by glycolipid-stimulated NKT cells, CpG ODN (27) was co-administered with OCH, in which IFN-γ production was preferentially augmented in response to IL-12 expression. CpG ODN induces innate immune responses similar to bacterial DNA, and is one of the PAMPs expressed by a diverse group of microorganisms. Taken together, a variety of glycolipid antigens elicit differential effects, not only on NKT cells but also on bystander cells such as NK cells and DCs, which may modulate subsequent immune responses. Recently, Brigl *et al.* demonstrated that a bacterial infection can induce a predominantly T_h1 cytokine responses from self-antigen-primed NKT cells. In this instance, microbial products were recognized not by NKT cells directly, but by DCs, resulting in IL-12 secretion and subsequent potent IFN-γ production (17). Following the exposure of immune cells to exogenous antigens or infection, IL-12 is produced by DCs in response to CD40 signals or microbial products, and co-stimulates the responses of NKT cells to self-antigens, resulting in a significant augmentation of IFN-γ production but no detectable IL-4 production (40). It is noteworthy to point out that the behavior of OCH in response to IL-12 is analogous to that of the putative self-antigen for NKT cells (Fig. 6). Therefore, NKT cells also respond to OCH in a diverse manner according to the availability of IL-12, which can be induced by a wide variety of pathogens, and thus OCH may be a useful tool to evaluate the physiological responses of NKT cells to various innate immune conditions.

Regarding the predominant effect of OCH on T_h2 polarization by NKT cells, several molecules have been identified that positively regulate T_h2 polarization, such as thymus-specific lymphopoietin (TSLP), OX40 ligand (OX40L) or prostaglandin (PG) E_2. In the microarray analysis of glycolipid-stimulated NKT cells and DCs, no inducible transcription of TSLP and OX40L in NKT cells was observed 1.5 or 12 h after OCH treatment. Furthermore, synthetic pathway for PGs seems quiescent because the expression of PG H synthetase (or cyclooxygenase 2), a key enzyme initiating PG synthesis, was not induced in either NKT cells or DCs after treatment with OCH. Considering that all of these molecules are regulated transcriptionally upon stimulation, the involvement of these molecules for OCH-mediated T_h2 polarization seems minimum. Taken together, the results demonstrated in this study suggest that OCH induces T_h2 predominance by a default pathway.

In summary, we have demonstrated here that OCH-mediated dominant T_h2 polarization is accomplished not only by the preferential IL-4 induction by NKT cells but also by the evasion of the secondary IFN-γ burst. This effect of OCH is due to the ineffective induction of IFN-γ and CD40L by NKT cells and the subsequent reduction of IL-12 secretion. These results demonstrate the cellular mechanisms involved in altered glycolipid ligand (OCH)-induced T_h2 polarization and immune regulation *in vivo*. Therefore, proper assessment of the effects of the innate immune system on the host's response should be taken into consideration when modulating NKT responses *in vivo* by glycolipids, such as OCH.

Acknowledgements

We thank Miho Mizuno for technical assistance and Yuki Kikai for cell sorting. We are grateful to John Ludovic Croxford for critical reading of the manuscript. This work was supported by the Pharmaceutical and Medical Devices Agency, Grant-in-Aid for Scientific Research (B) 14370169 from Japan Society for the Promotion of Science, Kato Memorial Bioscience Foundation and Uehara Memorial Foundation.

Abbreviations

APC	allophycoerythrin
CD40L	CD40 ligand
CIA	collagen-induced arthritis
DC	dendritic cell
EAE	experimental autoimmune encephalomyelitis
Flt3L	Flt3-ligand
αGC	α-Galactosylceramide
iNKT	invariant NKT
NF-κB	nuclear factor-κB
ODN	oligodeoxynucleotide
OX40L	OX40 ligand
PAMP	pathogen-associated molecular pattern
PG	prostaglandin
TSLP	thymus-specific lymphopoietin

References

1 Kronenberg, M. and Gapin, L. 2002. The unconventional lifestyle of NKT cells. *Nat. Rev. Immunol.* 2:557.
2 Taniguchi, M., Harada, M., Kojo, S., Nakayama, T. and Wakao, H. 2003. The regulatory role of Valpha14 NKT cells in innate and acquired immune response. *Annu. Rev. Immunol.* 21:483.
3 Smyth, M. J., Crowe, N. Y., Pellicci, D. G. *et al.* 2002. Sequential production of interferon-gamma by NK1.1(+) T cells and natural killer cells is essential for the antimetastatic effect of alpha-galactosylceramide. *Blood* 99:1259.
4 Singh, N., Hong, S., Scherer, D. C. *et al.* 1999. Cutting edge: activation of NK T cells by CD1d and alpha-galactosylceramide directs conventional T cells to the acquisition of a Th2 phenotype. *J. Immunol.* 163:2373.
5 Hayakawa, Y., Takeda, K., Yagita, H., Van Kaer, L., Saiki, I. and Okumura, K. 2001. Differential regulation of Th1 and Th2 functions of NKT cells by CD28 and CD40 costimulatory pathways. *J. Immunol.* 166:6012.
6 Mizuno, M., Masumura, M., Tomi, C. *et al.* 2004. Synthetic glycolipid OCH prevents insulitis and diabetes in NOD mice. *J. Autoimmun.* 23:293.
7 Chiba, A., Oki, S., Miyamoto, K., Hashimoto, H., Yamamura, T. and Miyake, S. 2004. Suppression of collagen-induced arthritis by natural killer T cell activation with OCH, a sphingosine-truncated analog of alpha-galactosylceramide. *Arthritis Rheum.* 50:305.
8 Miyamoto, K., Miyake, S. and Yamamura, T. 2001. A synthetic glycolipid prevents autoimmune encephalomyelitis by inducing TH2 bias of natural killer T cells. *Nature* 413:531.
9 Oki, S., Chiba, A., Yamamura, T. and Miyake, S. 2004. The clinical implication and molecular mechanism of preferential IL-4 production by modified glycolipid-stimulated NKT cells. *J. Clin. Investig.* 113:1631.
10 Carnaud, C., Lee, D., Donnars, O. *et al.* 1999. Cross-talk between cells of the innate immune system: NKT cells rapidly activate NK cells. *J. Immunol.* 163:4647.
11 Fujii, S. I., Shimizu, K., Smith, C., Bonifaz, L. and Steinman, R. M. 2003. Activation of natural killer T cells by {alpha}-galactosylceramide rapidly induces the full maturation of dendritic cells *in vivo* and thereby acts as an adjuvant for combined CD4 and CD8 T cell immunity to a coadministered protein. *J. Exp. Med.* 198:267.
12 Hermans, I. F., Silk, J. D., Gileadi, U. *et al.* 2003. NKT cells enhance CD4+ and CD8+ T cell responses to soluble antigen *in vivo* through direct interaction with dendritic cells. *J. Immunol.* 171:5140.
13 Kitamura, H., Ohta, A., Sekimoto, M. *et al.* 2000. Alpha-galactosylceramide induces early B-cell activation through IL-4 production by NKT cells. *Cell Immunol.* 199:37.
14 Schmieg, J., Yang, G., Franck, R. W. and Tsuji, M. 2003. Superior protection against malaria and melanoma metastases by a C-glycoside analogue of the natural killer T cell ligand alpha-galactosylceramide. *J. Exp. Med.* 198:1631.
15 Vincent, M. S., Leslie, D. S., Gumperz, J. E., Xiong, X., Grant, E. P. and Brenner, M. B. 2002. CD1-dependent dendritic cell instruction. *Nat. Immunol.* 3:1163.
16 Tomura, M., Yu, W. G., Ahn, H. J. *et al.* 1999. A novel function of Valpha14+CD4+NKT cells: stimulation of IL-12 production by antigen-presenting cells in the innate immune system. *J. Immunol.* 163:93.
17 Brigl, M., Bry, L., Kent, S. C., Gumperz, J. E. and Brenner, M. B. 2003. Mechanism of CD1d-restricted natural killer T cell activation during microbial infection. *Nat. Immunol.* 4:1230.
18 Gilliet, M., Boonstra, A., Paturel, C. *et al.* 2002. The development of murine plasmacytoid dendritic cell precursors is differentially regulated by FLT3-ligand and granulocyte/macrophage colony-stimulating factor. *J. Exp. Med.* 195:953.
19 Chiba, A., Kaieda, S., Oki, S., Yamamura, T. and Miyake, S. 2005. The involvement of V(alpha)14 natural killer T cells in the pathogenesis of arthritis in murine models. *Arthritis Rheum.* 52:1941.
20 Pal, E., Tabira, T., Kawano, T., Taniguchi, M., Miyake, S. and Yamamura, T. 2001. Costimulation-dependent modulation of experimental autoimmune encephalomyelitis by ligand stimulation of V alpha 14 NK T cells. *J. Immunol.* 166:662.
21 Kitamura, H., Iwakabe, K., Yahata, T. *et al.* 1999. The natural killer T (NKT) cell ligand alpha-galactosylceramide demonstrates its immunopotentiating effect by inducing interleukin (IL)-12 production by dendritic cells and IL-12 receptor expression on NKT cells. *J. Exp. Med.* 189:1121.
22 Trinchieri, G. 2003. Interleukin-12 and the regulation of innate resistance and adaptive immunity. *Nat. Rev. Immunol.* 3:133.
23 Schulz, O., Edwards, A. D., Schito, M. *et al.* 2000. CD40 triggering of heterodimeric IL-12 p70 production by dendritic cells *in vivo* requires a microbial priming signal. *Immunity* 13:453.
24 Hilkens, C. M., Kalinski, P., de Boer, M. and Kapsenberg, M. L. 1997. Human dendritic cells require exogenous interleukin-12-inducing factors to direct the development of naive T-helper cells toward the Th1 phenotype. *Blood* 90:1920.
25 Vieira, P. L., de Jong, E. C., Wierenga, E. A., Kapsenberg, M. L. and Kalinski, P. 2000. Development of Th1-inducing capacity in myeloid dendritic cells requires environmental instruction. *J. Immunol.* 164:4507.
26 Snijders, A., Kalinski, P., Hilkens, C. M. and Kapsenberg, M. L. 1998. High-level IL-12 production by human dendritic cells requires two signals. *Int. Immunol.* 10:1593.
27 Klinman, D. M. 2004. Immunotherapeutic uses of CpG oligodeoxynucleotides. *Nat. Rev. Immunol.* 4:249.
28 Krug, A., Towarowski, A., Britsch, S. *et al.* 2001. Toll-like receptor expression reveals CpG DNA as a unique microbial stimulus for plasmacytoid dendritic cells which synergizes with CD40 ligand to induce high amounts of IL-12. *Eur. J. Immunol.* 31:3026.
29 Parekh, V. V., Singh, A. K., Wilson, M. T. *et al.* 2004. Quantitative and qualitative differences in the *in vivo* response of NKT cells to distinct alpha- and beta-anomeric glycolipids. *J. Immunol.* 173:3693.
30 Goff, R. D., Gao, Y., Mattner, J. *et al.* 2004. Effects of lipid chain lengths in alpha-galactosylceramides on cytokine release by natural killer T cells. *J. Am. Chem. Soc.* 126:13602.
31 Smyth, M. J., Thia, K. Y., Street, S. E. *et al.* 2000. Differential tumor surveillance by natural killer (NK) and NKT cells. *J. Exp. Med.* 191:661.
32 Whiteside, T. L. and Herberman, R. B. 1995. The role of natural killer cells in immune surveillance of cancer. *Curr. Opin. Immunol.* 7:704.
33 Ortaldo, J. R., Young, H. A., Winkler-Pickett, R. T., Bere, E. W., Jr, Murphy, W. J. and Wiltrout, R. H. 2004. Dissociation of NKT stimulation, cytokine induction, and NK activation *in vivo* by the use of distinct TCR-binding ceramides. *J. Immunol.* 172:943.

34 Ueno, Y., Tanaka, S., Sumii, M. *et al.* 2005. Single dose of OCH improves mucosal T helper type 1/T helper type 2 cytokine balance and prevents experimental colitis in the presence of valpha14 natural killer T cells in mice. *Inflamm. Bowel Dis.* 11:35.
35 Cella, M., Scheidegger, D., Palmer-Lehmann, K., Lane, P., Lanzavecchia, A. and Alber, G. 1996. Ligation of CD40 on dendritic cells triggers production of high levels of interleukin-12 and enhances T cell stimulatory capacity: T-T help via APC activation. *J. Exp. Med.* 184:747.
36 Quezada, S. A., Jarvinen, L. Z., Lind, E. F. and Noelle, R. J. 2004. CD40/CD154 interactions at the interface of tolerance and immunity. *Annu. Rev. Immunol.* 22:307.
37 Hayes, M. P., Murphy, F. J. and Burd, P. R. 1998. Interferon-gamma-dependent inducible expression of the human interleukin-12 p35 gene in monocytes initiates from a TATA-containing promoter distinct from the CpG-rich promoter active in Epstein–Barr virus-transformed lymphoblastoid cells. *Blood* 91:4645.
38 Ma, X., Chow, J. M., Gri, G. *et al.* 1996. The interleukin 12 p40 gene promoter is primed by interferon gamma in monocytic cells. *J. Exp. Med.* 183:147.
39 Grohmann, U., Belladonna, M. L., Bianchi, R. *et al.* 1998. IL-12 acts directly on DC to promote nuclear localization of NF-kappaB and primes DC for IL-12 production. *Immunity* 9:315.
40 Gumperz, J. E. 2004. CD1d-restricted NKT cells and myeloid IL-12 production: an immunological crossroads leading to promotion or suppression of effective anti-tumor immune responses? *J. Leukoc. Biol.* 76:307.

ARTHRITIS & RHEUMATISM
Vol. 52, No. 6, June 2005, pp 1941–1948
DOI 10.1002/art.21056

The Involvement of $V_\alpha 14$ Natural Killer T Cells in the Pathogenesis of Arthritis in Murine Models

Asako Chiba, Shinjiro Kaieda, Shinji Oki, Takashi Yamamura, and Sachiko Miyake

Objective. **To examine the physiologic role of natural killer T (NKT) cells bearing $V_\alpha 14$ T cell receptor (TCR) in the pathogenesis of collagen-induced arthritis (CIA) and antibody-induced arthritis in mice.**

Methods. **NKT cells were stained with α-galactosylceramide–loaded CD1 dimer, and then assessed using flow cytometry. CIA was induced in mice by immunization on days 0 and 21 with type II collagen (CII) emulsified with an equal volume of Freund's complete adjuvant. Anti-CII antibodies were measured by enzyme-linked immunosorbent assay. For antibody-induced arthritis, mice were injected with anti-CII monoclonal antibodies (mAb) followed by lipopolysaccharide, or with serum from KRN TCR–transgenic mice crossed with nonobese diabetic mice (K/BxN). The severity of arthritis was monitored with a macroscopic scoring system.**

Results. **The number of NKT cells increased in the liver at the peak of the clinical course of CIA. Administration of anti-CD1 mAb inhibited development of CIA. The severity of CIA in NKT cell–deficient mice was reduced compared with that in wild-type mice. The IgG1:IgG2a ratio of anti-CII was elevated and production of interleukin-10 from draining lymph node cells was increased in NKT cell–deficient mice. NKT cell–deficient mice were significantly less susceptible to antibody-induced arthritis.**

Conclusion. **NKT cells contribute to the pathogenesis of arthritis by enhancing autoantibody-mediated inflammation. NKT cells also contribute to the disease process in a deleterious way, due, at least in part, to the alteration of the Th1/Th2 balance in T cell response to CII.**

Rheumatoid arthritis (RA) is a common autoimmune disease characterized by persistent inflammation of the joints. Affected joints display hyperplasia of the synovia with large cellular infiltrates of several cell types, including neutrophils, macrophages, T cells, B cells, dendritic cells, and fibroblasts. Complement deposition and high levels of proinflammatory cytokine expression are found in the synovial and periarticular regions, and the perpetuation of synovitis results in destruction of the cartilage and bone of the affected joints. Although the etiology of RA remains controversial, cumulative evidence suggests that T cell–mediated autoimmune responses play an important role, and the ensuing inflammation is a critical component in the processes leading to damage of joint cartilage and bone (1).

Natural killer T (NKT) cells are a unique subset of T cells that coexpress receptors of the NK lineage and α/β T cell receptor (TCR). A majority of NKT cells express an invariant TCRα chain (encoded by a $V_\alpha 14$–$J_\alpha 281$ rearrangement in mice and a homologous $V_\alpha 24$–$J_\alpha Q$ rearrangement in humans). Unlike conventional T cells that recognize peptides in association with the major histocompatibility complex (MHC), $V_\alpha 14$ NKT cells recognize glycolipid antigens such as α-galactosylceramide (α-GC) presented by the nonpolymorphic MHC class I–like protein, CD1d. $V_\alpha 14$ NKT cells have been demonstrated to regulate a variety of immune responses through their capacity to produce a large amount of cytokines, including interleukin-4 (IL-4) and interferon-γ (IFNγ), in response to TCR ligation or cytokine stimulation (2–4). Furthermore, we previously demonstrated that stimulation of $V_\alpha 14$ NKT cells with the glycolipid ligand, OCH, can inhibit collagen-induced arthritis (CIA), a murine experimental model for RA

Supported by a grant-in-aid for scientific research from the Japan Society for the Promotion of Science (B-14370169), the Uehara Memorial Foundation, the Kato Memorial Bioscience Foundation, and the Pharmaceutical and Medical Devices Agency.

Asako Chiba, MD, PhD, Shinjiro Kaieda, MD, Shinji Oki, PhD, Takashi Yamamura, MD, PhD, Sachiko Miyake, MD, PhD: National Institute of Neuroscience, Tokyo, Japan.

Address correspondence and reprint requests to Sachiko Miyake, MD, PhD, Department of Immunology, National Institute of Neuroscience, NCNP 4-1-1 Ogawahigashi, Kodaira, Tokyo 187-8502, Japan. E-mail: miyake@ncnp.go.jp.

Submitted for publication July 30, 2004; accepted in revised form March 1, 2005.